ULTRASONIC REFLECTION MODE TOMOGRAPHY USING FREQUENCY SHIFTED METHOD

THONGSAMLID ONEMANISONE

A THESIS SUBMITTED IN PARTIAL FULFILMENT

OF THE REQUIREMENT FOR THE DEGREE OF

MASTER ENGINEERING IN ELECTRONICS ENGINEERING

SCHOOL OF GRADUATE STUDIES

KING MONGKUT'S INSTITUTE OF TECHNOLOGY LADKRABANG

2007

Table of Contents

Table of Contents (Cont.)

List of Tables

List of Figures

List of Figures (Cont.)

List of Figures (Cont.)

หัวข้อวิทยานิพนธ์	การสร้างภาพตัดขวางในโหมดสะท้อนด้วยคลื่นอัลตร้าโซนิค โดยใช้เทคนิคการเลื่อนของความถี่
นักศึกษา	นายทองสัมลิด อ่อนมะนีสอน
รหัสนักศึกษา	48060421
ปริญญา	วิศวกรรมศาสตรมหาบัณฑิต
สาขาวิชา	วิศวกรรมอิเล็กทรอนิกส์
พ.ศ.	2550
อาจารย์ผู้ควบคุมวิทยานิพนธ์	รศ.ดร.มนัส สังวรศิลป์
อาจารย์ผู้ควบคุมวิทยานิพนธ์ร่วม	รศ.ดร.ชูชาติ ปิณฑวิรุจน์

บทคัดย่อ

โทโมกราฟฟีคือกระบวนการสร้างภาพตัดขวางของวัตถุโดยไม่ทำให้วัตถุเสียหาย ข้อมูลดิบของกระบวนการนี้ถูกเรียกว่าภาพโปรเจคชัน ซึ่งโดยปกติแล้วได้มาจากการแผ่คลื่นในย่านความถี่จำกัดทะลุผ่านวัตถุที่มุมต่างๆกันแล้วรับด้วยแผงของตัวรับคลื่นในด้านตรงข้าม สำหรับงานวิจัยนี้การสร้างภาพตัดขวางของวัตถุสามารถทำได้โดยการใช้ข้อมูลโปรเจคชันจากการยิงคลื่นอัลตร้าโซนิคผ่านเนื้อเยื่อวัตถุ ขณะที่ข้อมูลจากการสร้างภาพตัดขวางในโหมดส่งผ่านด้วยคลื่นอัลตร้าโซนิคไม่สามารถสร้างรายระเอียดของเนื้อเยื่อที่เกิดจากเงาสะท้อนของกระดูกได้ การสร้างภาพตัดขวางในโหมดสะท้อนด้วยคลื่นอัลตร้าโซนิคได้ถูกนำมาใช้เพื่อแก้ไขปัญหานี้ ในการสร้างข้อมูลโปรเจคชันนั้นสามารถทำได้หลายวิธี วิธีการหาค่าสัมประสิทธิ์การลดทอนของคลื่นอัลตร้าโซนิคจากการยิงผ่านเนื้อเยื่อวัตถุ วิธีเหล่านี้ ได้รับการพิสูจน์มาแล้วจากสัญญาณข้อมูลที่ได้รับจากการส่งผ่านคลื่นอัลตร้าโซนิคผ่านเนื้อวัตถุ แต่อย่างไรก็ตามก็ยังสามารถปรับใช้ข้อดีจากวิธีเหล่านั้นเพื่อให้เข้ากับโหมดสะท้อนได้ทำการใช้เทคนิคการเลื่อนของความถี่มาใช้ เนื่องจากข้อดีของเทคนิคดังกล่าวในเชิงการคำนวณ อัลกอริธึมที่ใช้ในกระบวนการสร้างภาพย้อนกลับของเนื้อเยื่อที่ถูกแทรกจากกระดูกได้แก่ ฟิลเตอร์แบ็กโปรเจคชันอัลกอริธึมอย่างง่าย ผลการสร้างภาพย้อนกลับจากข้อมูลการเลื่อนของความถี่ได้รับการแสดงค่าเหนือกว่าการสร้างภาพตัดขวางในโหมดส่งผ่านด้วยคลื่นอัลตร้าโซนิค อีกทั้งการจำลองสำหรับสัญญาณรบกวนก็ได้รับการวิเคราะห์ด้วย.

Thesis Title	Ultrasonic Reflection Mode Tomography using Frequency Shifted Method
Student	Mr.Thongsamlith Onemanisone
Student ID.	48060421
Degree	Master of Engineering
Programme	Electronics Engineering
Year	2007
Thesis Advisor	Assoc.Prof.Dr.Manas Sangworasil
Thesis Co-Advisor	Assoc.Prof.Dr.Chuchart Pintavirooj

ABSTRACT

Tomographic imaging is a technique for exploring a cross-section of an inspected object without destruction it. Raw data of this process, known as the projections, are normally achieved by repeatedly radiating coherent waveforms through the object in a number of viewpoints, and receiving them using an array of corresponding detector in the same direction. In this thesis of tissue reconstruction can be reconstructed by using its projections resolved from the ultrasonic broadband wave which is passed through the tissue. While a data from ultrasonic transmission-mode tomography can not be used to image the character of tissue where shadowed by a bone, an ultrasonic reflection-mode tomography is realized to be a solution for this. There are many ways to extract the projections by using the integrated attenuation coefficients of the tissue from the pulse wave. Almost all of these methods were proved to implement with the transmission-mode signals, but however, some adaptation may takes benefit from those methods to implement with the reflection-mode. We have chosen the frequency-shifted method to be analyzed because of its advantage in a computational viewpoint. This simple filtered backprojection algorithm was implemented to reconstruct the tomographic images of the tissue suffered by bone. The results are shown the successful of this method over the transmission-mode tomography. Also the simulations for noisy data were analyzed.

Acknowledgements

Along the great journey of this master thesis, I have been facing with both the hard times and the good times. Someone helped me in the hard times, someone applauded me in the good times, and someone encouraged me while I felt desperate. Without them, I would not have made it this far. At this point, I would like to express my appreciation to these companions.

My parents for being supportive in everything, and both of them are always the heroes for me. My great advisors, Assoc.Prof.Dr. Manas Sangworasil and Assoc.Prof.Dr. Chuchart Pintavirooj, for giving me a great deal and ideas of invaluable suggestions and concepts, including the heart of being a good researcher. Assist.Prof.Dr. Kitiphon Chitsakul, Assoc.Prof.Dr. Surapan Airphaiboon for their helpful comments both in and out of the course. Assist.Prof. Arthorn Sanpanich for assembling the significant English.

Special thanks the Assoc. Prof. Dr. Jongkol Ngamwiwit for a honor teaching on studying in King Mongkut's Institute of Technology Ladkrabang (KMITL). Mr. Walita Narkbuakaew for guiding me the basic principle of MATLAB7 and programming techniques tips, and sharing me the workplace. Mr.Kata Jaruwongrungsee for providing much assistance along my first step. The senior staffs of Biomedical Signal and Image Processing laboratory and Research Center for Communication and Information Technology (ReCCIT) staffs for their helpfulness.

Most of my researching fund has been kindly supported by ASEAN University Network/Southeast Asia Engineering Education Development Network (AUN/SEED-Net), Japan International Cooperation Agency (JICA) project and the Faculty of engineering, KMITL.

Thongsamlid Onemanisone

Chapter 1

Introduction

1.1 Significance of the Problem

Ultrasound is a mechanical disturbance that moves as a pressure wave through a medium. When the medium is a patient, the wavelike disturbance is the basis for use of ultrasound as a diagnostic tool. Appreciation of the characteristics of ultrasound waves and their behavior in various media is essential to understanding the use of diagnostic ultrasound in clinical medicine.

Just on the horizon there is yet another tomographic imaging mode currently undergoing clinical trials. This is the technique of ultrasonic computed tomography (UCT). The basic goal here is the same as with X-rays, namely, to obtain quantitative cross-sectional images depicting morphological detail of the human body. However, in contrast with X-rays, CT imaging with ultrasound is made difficult by the fact that rays of sound's energy do not necessarily travel along straight lines in tissue, and may undergo serious refraction at interfaces between soft and hard tissues. On account of this, applications of ultrasound CT appear to be limited for the foreseeable future to those parts of human body that are free of hard tissues such as bone. Thus most of the current effort in this area is focused on the clinically important problem of tumor detection in the female breast.

Ultrasound has a potentially many important technological applications. These include medical imaging [1], nondestructive testing [2], geophysics [3], and robotic vision [2]. The advantages of microwave and/or ultrasound imaging offered over more conventional imaging are numerous. They include the relatively low health hazard of non-ionizing, low power of sources, such as microwave, ultrasound, etc., its ability to image physiological properties of a tissue or organ, and the likely cost competitiveness of the imaging equipment.

In ultrasound imaging, conventional B-scan image use pulse echo ultrasound reflected from tissue interface to form image as tomography. Pulse-echo B-scan image is not quantitative imaging. Work is now progress on methods of correlating (quantitatively) these scattered returns with local properties of tissue [4-5]. This is made difficult by the fact that the scattered returns are modified every time they pass through an interface; hence the interest in computed ultrasonic tomography as an alternative strategy for quantitative imaging with sound. This is mainly due to the fact that ultrasonic computed tomography (UCT) may generate cross-sectional images (tomograms) of three different material properties: (I) an attenuation tomogram representing the ultrasonic energy loss due to scatter and absorption in the material; (ii) a speed-of-sound tomogram representing a measure of the elastic constants in the material [6]; and, (iii) a reflection tomogram representing a map of ultrasonic impedance mismatch from boundaries and in homogeneities. As a result, ultrasonic computed tomography now receives an intensive attention from many researchers.

Ultrasonic mode can be classified into 2 modes; reflection mode and transmission mode. Reflection mode is the technique that uses one ultrasonic transducer head which set opposite the object and functioned as transmitter and receiver in one head. But in transmission mode; two ultrasonic transducer heads work separately as two functions; one is functioned as transmitter and the other one is functioned as receiver*. Both of transmitter and receiver are set at opposite sites; one is forward site (transmitter), other one is backward site (receiver) objects respectively.

In addition, both of two sources for ultrasonic tomography are non-diffraction ultrasonic tomography and diffraction ultrasonic tomography; but in our research only first source is used. Diffraction ultrasonic tomography is a tomography that needs to compensate an ultrasonic diffractive index values. In addition, this tomography is used for compensating the diffractive indexes passed through the objects during reconstruction procedure. Moreover, nondiffraction ultrasonic tomography is a tomography that does not need to compensate an ultrasonic diffractive index values; this tomography is used for noncompensating the diffractive indexes passed through the objects during reconstruction procedure. Finally, reflection/transmission mode diffraction/nondiffraction ultrasonic tomography can be introduced as following:

- Reflection / transmission mode diffraction ultrasonic tomography
- Reflection / transmission mode nondiffraction ultrasonic tomography

Firstly, reflection/transmission mode diffraction ultrasonic tomography is a tomography that needs to compensate an ultrasonic diffractive index values. This tomography is used for compensating the diffractive indexes objects during the reconstruction procedure. Diffraction tomography reviewed by Dr.Chuchart Pintavirooj [20]. Diffraction tomography is a technique for imaging with acoustic fields in which parameter, such as reflective index, sound velocity, etc., can be mapped from scatter wave resulting from insonifying the object with ultrasonic pulse wave at a single temporal frequency (3.5 MHz for simulation and 5 MHz for experimental processes). By solving the direct scattering problem, the scattered field can be presented in term of scattering parameters. Different inversion techniques can be applied to take advantage of the linearization process of the non-linear wave equation describing wave propagation in heterogeneous media under for limited class of scattering. Specifically, when the scattering effect is weak, one can invoke the Born or Rytov approximation and thus derive the generalized Fourier slice theorem to reconstruct the cross-section of the insonified object.

Secondly, reflection/transmission mode nondiffraction ultrasonic tomography is a tomography that does not need to compensate an ultrasonic diffractive index values. This tomography is used for noncompensating the diffractive indexes objects during the reconstruction procedure. Nondiffraction tomography reviewed by [20]. Nondiffraction tomography is a tomography which the diffraction effect of scattered filed is disregarded [8], an object is insonified with ultrasonic pulse waves, the Fourier transform of the forward scattering fields measured in a line perpendicular to the direction of propagation of the wave gives the values of the 2D Fourier Transform [19] of the object along a straight line. This is in fact the well-known Fourier slice theory and can be implemented using filtered backprojection.

Recall, transmission mode tomography is a tomography that needs two transducers to be aligned in optimum-position*. In addition, the transmission mode tomography system is more complex and it is not clinical practice because the object is needed to submerge in the water.

In this research we attempted to develop reflection mode tomography, it is superior to the transmission mode in the following reasons: (i) we use only one transducer (transmitter/receiver are contained in one element), (ii) the system of transmission is more complex, because they need two transducers aligned in the optimal position, (iii) the price of the equipments of transmission mode is higher than the equipments of reflection mode. In addition, two ultrasonic transducers of transmission mode tomography system; one (transmitter) is used for transmitting ultrasonic pulse waves. The other one (receiver**) is used for receiving ultrasonic pulse waves; the received ultrasonic pulse waves are obtained from insonifying an object.

In addition, we also concentrate about ultrasonic tomographic imaging for non-diffracting source which uses frequency-shifted method for extracting the projections. - Ultrasonic reflection mode tomography using frequency-shifted method. The frequency shifting method, firstly purposed by [18] for the transmission mode tomography, is employed to extract the integrated attenuation coefficient from the reflected ultrasonic pulse wave. This method assumes the linear frequency dependent model of the attenuation coefficient.

Note: * = the centre of transducer heads must be matched altogether.

** = (the receiver can be call hydrophone).

1.2 Objective

The objectives of this research can be shown as following,

1. The advantages of reflection mode ultrasonic computed tomography is introduced.
2. Cross-sectional image/object reconstruction by reflection mode ultrasonic computed tomography is introduced.
3. A frequency-shifted method is introduced and applied for "reflection mode ultrasonic computed tomography uses frequency-shifted method" for obtaining the projection data.
4. All simulation and experiment results are displayed (in chapter 5).

1.3 Hypothesis

Reflection mode of UCT is valid, if an object has small changes in refractive index. In addition, if we calculate the exact scattered pulse wave for a small and weakly scattering object we can assume that the obtained projections from a small changes in refractive index is exact. The obtained cross-sectional image results are acceptable from this method.

In a process of reflection mode ultrasonic computed tomography can be ranked as following:

1. In ultrasonic computed tomography, if there is a small change in diffractive index of the object we can assume the wave traveling as a direct wave and we take the data to reconstruct a cross section of the object. This method is known as nondiffraction source.

2. Any objects that we want to scan can be tested by measuring the reflected ultrasonic wave pulses displayed on oscilloscope.

2. Projections can be obtained by computing the different spectral frequency values between the incident wave pulses and the latest wave pulses and dividing them by invariance values.

3. For the acceptable reconstructed image requirement, the angles of collecting the projections should be sufficient angular.

4. Simple homogenous object model are required for testing the system and reconstructed object modes.

1.4 Research Limits

The limitations of our research are shown as following reasons:

1. Nondiffraction data shows only acceptable reconstructed results
2. The object size is limited by transducer scanning length.
3. Cross-sectional object imaging from ultrasonic reflection mode using frequency-shifted method is satisfactory results
4. The reconstructed results from simulation and experiment are shown in the different of objects.
5. A *filtered Backprojection* algorithm [7] is applied to reconstruct the projections from both data of ultrasonic simulation and experiment.
6. A small detail of object information is necessary for high diffractive index soft tissue. To solve this problem a diffraction projections are realized to study in the future.

Chapter 2

The Ultrasonic General Information

This chapter exactly contains the principle of ultrasound (ultrasonic wave) and other topics such as: what is ultrasound (ultrasonic wave), why we use an ultrasonic wave, how does an ultrasonic wave work. Other related topics to the previous existed topics are following: the ultrasonic transducer and its applications, the principles of ultrasonic transducer, piezoelectric effect basics, impulse echo method. In addition, this chapter would include the acoustic properties of biological tissue, some examples of ultrasound application and medical diagnostic applications. For more information about ultrasonic principle see [9].

2.1 About Ultrasound

2.1.1 What is ultrasound?

Ultrasonic waves are unlike light and radio waves, sound waves require a medium for their transmission. The normal range of human hearing is approximately 20Hz - 20KHz. Ultrasonic wave is any sound with higher frequency. For more information about ultrasound in medical see [10].

Consider a sinusoidal sound wave in air with frequency f and wavelength λ. The speed v is related to f and λ by

$$v = f\lambda \tag{2.1}$$

To see where this relation comes from equation 2.2.

$$\text{speed} = \frac{\text{change in distance}}{\text{change in time}} \tag{2.2}$$

The time it takes for one wavelength of the sound to go by is the period T, so $v = \lambda/T$. But $f=1/T$ so $v = \lambda f$. Note that as f increases, λ goes down, but the speed v stays the same. The frequency range of human hearing is about 20 Hz to 20,000 Hz. (The upper end drops as we age; for people over 60*, it is about 12 kHz, while dogs can hear up to about 35 kHz.)

Note: * Are people; for over 60 persons/people is equal 12 kHz because a person can hear 5 kHz.

2.1.2 Why do we use an ultrasonic wave?

Ultrasonic wave is very safe. There is no firm evidence that it does any harm to the body or tissue that is issued by it. X-rays are potentially dangerous; particularly to young children and pregnant women (they damage the unborn baby). For more information about ultrasound in medical see [10].

We use ultrasonic waves because the wavelength is easily measured with an ordinary meter stick. Further more, the frequency of ultrasound is above the range of human hearing, so the experiment does not create an audible sound. The experiment also illustrates the interference of waves

2.1.2 How does an ultrasonic wave work?

Medical ultrasound systems use high frequencies - several megahertz (mega means million or 10^6). A sound is a wave which has all the usual wave properties (reflection, refraction, diffraction). Ultrasound imaging makes use of the fact that sound can be reflected. The idea is just like that used in radar and sonar. For more information about ultrasound in medical see [10].

In general, however, we speak of ultrasound whenever the sound frequency exceeds 20 kHz. Of course, the definition is in no way justified from a physical point of view, since the physical of sound production and propagation do not depend on frequency. Thus, practical methods of sound generation and sound detection substantially differ in general from those employed in the audible range.

2.2 An Ultrasonic Immersion Transducer

An immersion transducer is a single element longitudinal wave transducer acoustically matched to water [11]. It is specifically designed to transmit ultrasound in situations where the test part is partially or wholly immersed.

Fig. 2.1 Example of ultrasonic transducers

The figure 2.1 shows an example of various immersion ultrasonic transducers. Their shapes are depended on their applications. In our experimental system, an immersion ultrasonic transducers (v309-su-f) is applied. The model is listed in above figure.

2.2.1 Applications

- ❖ Automated scanning
- ❖ On-line thickness gagging
- ❖ High speed flaw detection in pipe, bar, tube, plate and other similar components
- ❖ Time-of-flight and amplitude based imaging
- ❖ Thru-transmission testing
- ❖ Material analysis and velocity measurements

2.2.2 Large diameter case style

- ❖ Large element diameters increase near field length allowing for longer focal lengths
- ❖ Larger diameters can increase scanning index

❖ Low frequency, large aperture designs available for challenging applications

2.3 About Ultrasonic Transducer

2.3.1 Piezoelectric effect basics

A piezoelectric substance is one that produces an electric charge when a mechanical stress is applied (the substance is squeezed or stretched). Conversely, a mechanical deformation (the substance shrinks or expands) is produced when an electric field is applied. This effect is formed in crystals that have no center of symmetry. To explain this, we have to look at the individual molecules that make up the crystal. Each molecule has a polarization, one end is more negatively charged and the other end is positively charged, and is called a dipole. This is a result of the atoms that make up the molecule and the way the molecules are shaped. The polar axis is an imaginary line that runs through the center of both charges on the molecule. In a monocrystal the polar axes of all of the dipoles lie in one direction. The crystal is said to be symmetrical because if you were to cut the crystal at any point, the resultant polar axes of the two pieces would lie in the same direction as the original. In a polycrystal, there are different regions within the material that have a different polar axis. It is asymmetrical because there is no point at which the crystal could be cut that would leave the two remaining pieces with the same resultant polar axis. Figure 2.2 illustrates this concept.

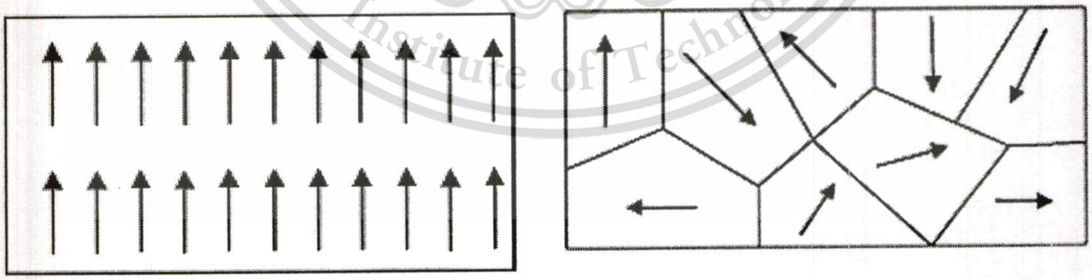

(a) Monocrystal with single polar axis (b) Polycrystal with random polar axis

Fig. 2.2 (a) Mono Vs. (b) Poly Crystals

In order to produce the piezoelectric effect, the polycrystal is heated under the application of a strong electric field. The heat allows the molecules to move more freely and the electric field forces all of the dipoles in the crystal to line up and face in nearly the same direction (Figure 2.3)

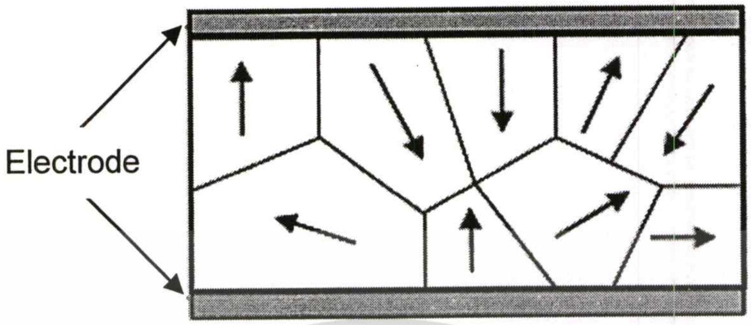

(a) Random Dipole

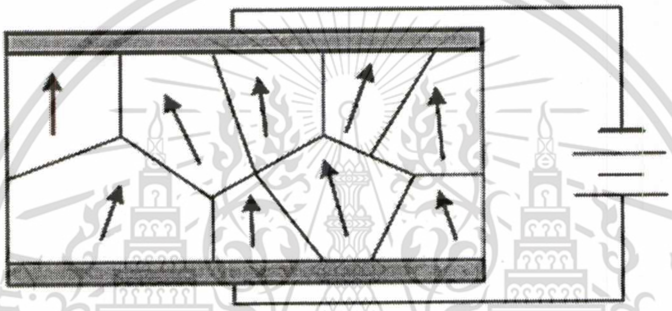

(b) Polarization

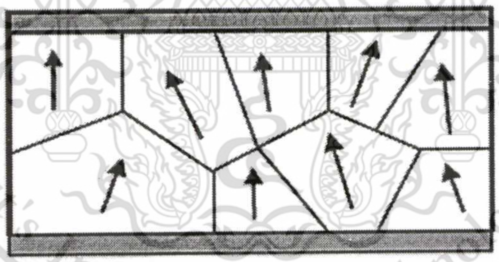

(c) Surviving Polarity

Fig. 2.3 Polarization of Ceramic Material to Generate Piezoelectric Effect

The piezoelectric effect can now be observed in the crystal. Figure 2.3 illustrates the piezoelectric effect.

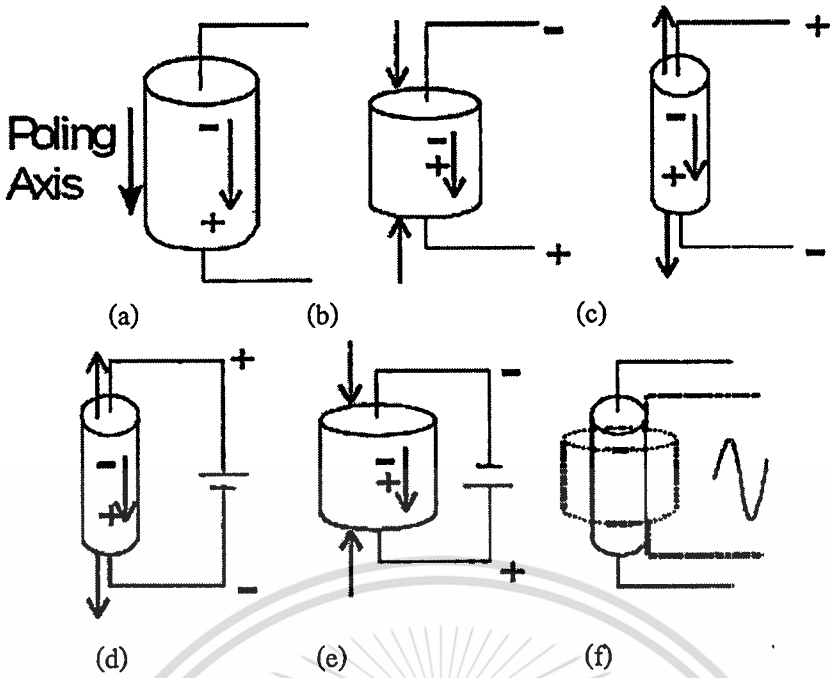

Fig. 2.4 Example of Piezoelectric Effect

Figure 2.4 (a) shows the piezoelectric material without a stress or charge. If the material is compressed, then a voltage of the same polarity as the poling voltage will appear between the electrodes (b). If stretched, a voltage of opposite polarity will appear (c). Conversely, if a voltage is applied the material will deform. A voltage with the opposite polarity as the poling voltage will cause the material to expand, (d), and a voltage with the same polarity will cause the material to compress (e). If an AC signal is applied then the material will vibrate at the same frequency as the signal (f).

2.3.2 Construction and function of the ultrasound

The construction and function of the ultrasound transducers used for the sonographic examination of patients are not very different from the testing units employed in non-destructive testing of materials. Acoustically, it is to be considered as a rigid piston oscillating with constant surface velocity. Hence, a rough idea of the geometry of the sound field produced by it can be obtained from figure 2.5.

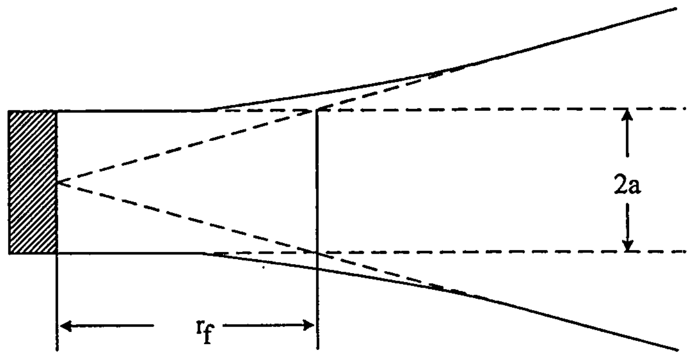

Fig. 2.5 Approximate extension of the sound field in front of a circular piston With ka>>1 (r_f = far field distance)

the far field distance r_f is approximately give by equation 2.3

$$r_f \approx \frac{S_0}{\lambda} \tag{2.3}$$

Where field distance r_f is equal to the area S_0 is divided by the wavelength λ respectively.

It has to be remembered, however, that for distances substantially smaller than r_f, i.e. in the near field of the transducer, considerable local fluctuations of the sound intensity are to be expected when the transducer if fed with a sine signal. If short impulses are p roduced the mentioned intensity fluctuations correspond to local differences of the impulse's shape. Since the impulse echo method generally employs one transducer both for the generation of the test signal and for its detection, the complicated spatial dependence of intensity for signal shape affects the signals twice. As in material testing, these near field effects can be avoided, at least in principle, by using a delay line, for instance a water layer between the transducer and the test object. In most cases, however, the number of different probing beams is chosen to be sufficiently high so as to ensure complete coverage of the region of interest.

2.4 Acoustic Properties of Biological Tissue

The inhomogeneities in the human body which are to be displayed with the aid of sonography are mostly the boundaries between different biological tissues and internal structures of tissues, in particular, of course, any pathological imperfections in them. Table 2.1 summarizes acoustical properties of some body tissues [7]. The data presented are the sound velocity, the characteristic impedance and the acoustical attenuation of various tissues at a frequency [12] which is typical for sonographic examination. As may be seen from this table, the characteristic impedances of soft biological tissues differs, only slightly form the characteristic impedance of water. Therefore, in contrast to what happens in the ultrasonic inspection of technical materials, only a very small fraction of a sound beam traversing an interface between such tissues will be reflected according to the equation followed,

$$R = \frac{Z_0' \cos\vartheta - Z_0 \cos\vartheta'}{Z_0' \cos\vartheta + Z_0 \cos\vartheta'} \tag{2.4*}$$

The "wall" under consideration is the boundary interface against another gaseous or liquid medium with sound velocity c' and characteristic impedance Z_o', a third wave appear, the 'refracted' wave. For the angle v' of refraction the following law holds

$$\frac{\sin v'}{\sin v} = \frac{C'}{C} \tag{2.5*}$$

Table 2.1** Acoustic Properties of Some Biological Tissues (after Bamber, 1986; Wells, 1969)

Kind of tissue	Sound Velocity c (m/s)	Characteristic impedance $\rho_0 c$ (10^6Ns/m^3)	Attenuation constant D at 1 MHz (dB/cm)
Blood	1530	1.62	0.2
Spleen	1550	1.6	0.4
Liver	1560	1.65	0.7
Fat	1450	1.38	0.8
Brain	1560	1.60	0.8
Muscle	1545-1630	1.65-1.74	1.5-2.5
Bone	2700-4100	3.2-7.4	11
Lung	650-1160	0.26-0.46	40
(Water)	1492	1.49	0.002

Note: * = equation 2.4 is from "Snell Law"

** = the acoustical properties of biological tissues are subject to strong differences. Therefore the data presented in this table should be considered as approximate only.

2.5 Impulse Echo Method and Its Usages

2.5.1 Impulse echo method

The principle of the impulse echo method which is encountered in the discussions on the measurement of sound velocity and sound absorption is explained in figure 2.6 reversible ultrasonic transducer emits a sound impulse or a short wave train into the work piece under test. At the same time the horizontal deflection of a cathode ray oscilloscope is triggered and the transducer is switched to the receiving circuit. If the test piece has a flat rear face, it will reflect the sound signal towards the transducer. The received signal is amplified, rectified and finally represented on the screen of the oscilloscope; it presents itself as a short peak (2). Another peak (0) is caused by electrical cross-talk between the transmitting and the receiving circuit. It marks, in effect, the beginning of the time axis. From the distance of both peaks, the transit time of the rear face signal and hence the thickness of the test piece may be determined if the sound velocity in the material is known. If there is an obstacle in the range covered by the emitted sound wave it will cause a scattered wave, part of which will also reach the transducer. Hence, an additional peak (1) will appear on the screen between both other peaks; its position indicates immediately the position of the defect in the test specimen.

It is one of the major advantages of the impulse echo method over transmission methods or testing procedures employing stationary signals that it indicates not only the existence of a defect but also its position. The same statement applies to transmission methods using other sorts of rays, for instance X-ray or gamma rays.

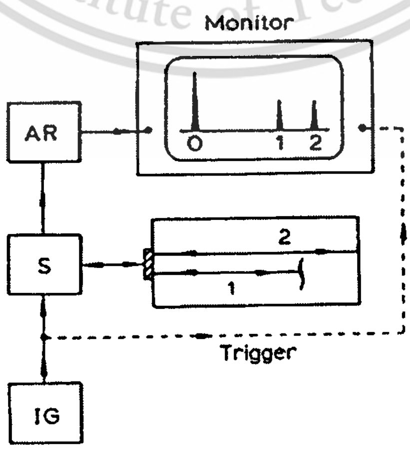

Fig. 2.6 Impulse echo method (IG, impulse generator; S, separating circuit; AR, amplifier and rectifier).

2.5.2 The uses of impulse echo method

The basic principle of the method is depicted in figure 2.6. In medical sonography, the impulse repetition rate is typically of the order of 1000/s. In most applications, the transducer is brought into direct contact with the surface of the body, only occasionally is the acoustical contact affected by means of a water bath. All the other processes—the excitation of the transducer with an electrical impulse, the transmission of a short wave train or acoustical impulse into the object of examination, which is the humans body in the present case, the detection of echoes and their display—are similar to those described earlier. Likewise, the discussions of Section 2.5.1 concerning the strength of echo signals apply to our present subject, although they have to be concluded by taking attenuation into account, which was neglected in Section 2.5.1.

2.6 Some Examples of Ultrasound Application

All of the sections present us about meaning and definition of ultrasound and also its application by material such piezoelectric transducers; another ultrasound application in industrial which are ultrasonic cleaning process which are up to date technique than the conventional techniques that we have to use solvent to clean the dirt particles.

Several example of ultrasound applications are will be represented in this sections which are following:

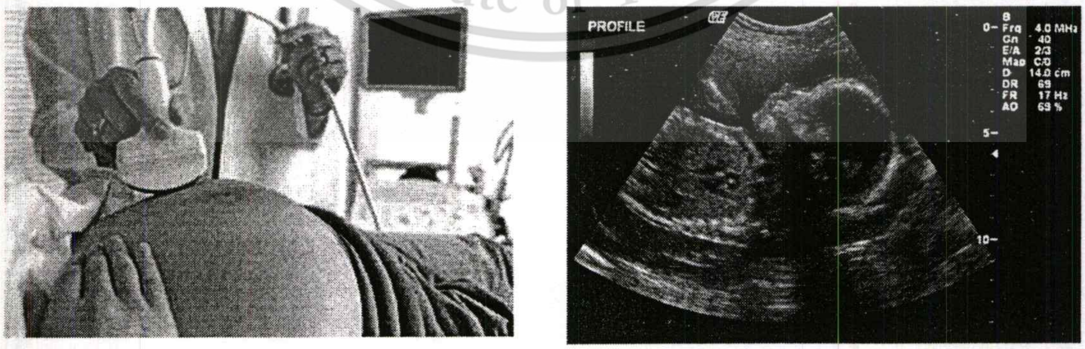

(a) (b)

Fig. 2.7 B-scan images of fetus; (a) transducers application, (b) fetus displaying

Another important applications, are the ultrasonic diagnostic applications such to check gall bladder, liver cancer, which can be able to known from the gray level of ultrasonic brightness. Other application of ultrasound is about fetus analysis before born, which is great technique to know firstly birth.

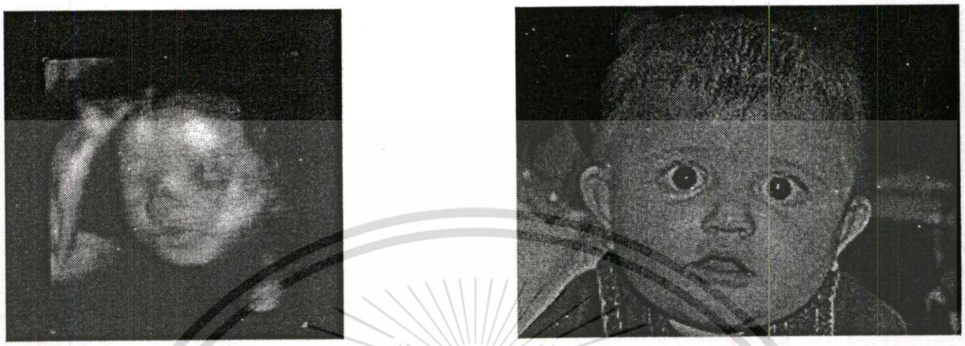

(a) (b)

Fig. 2.8 Image processing technique of fetus visualization (a) image model of ultrasound transducer (6^{th} month of pregnancy), (b) a child image (after real birth 6 months)

(a) (b)

Fig. 2.9 Ultrasound shows sector image of the gall bladder containing a stone;(a) Normal gallbladder, (b) Gallstone

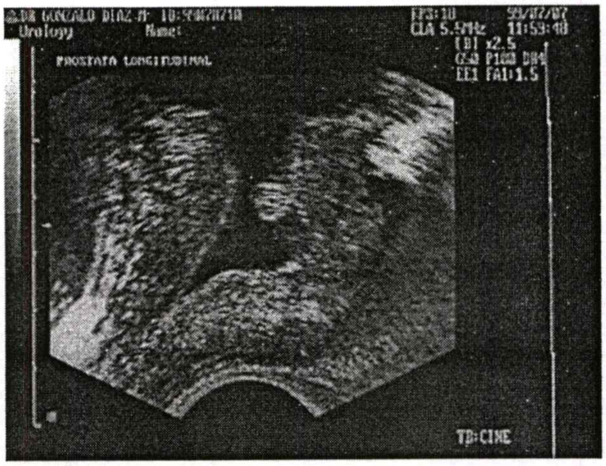

Fig. 2.10 Ultrasonic application to checks and images glandule cancer

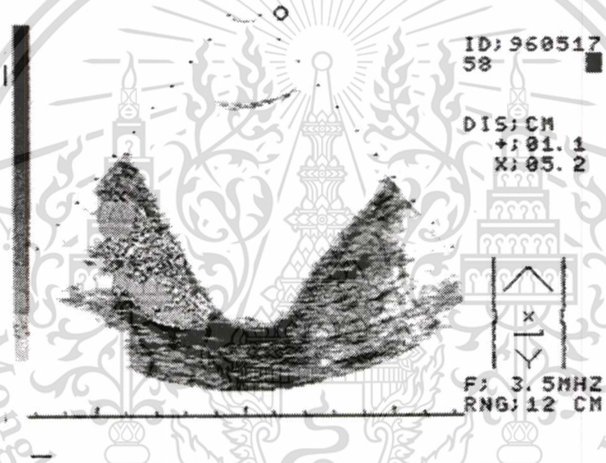

Fig. 2.11 Ultrasonic application to check ovary

Furthermore, there are also the applications of ultrasound in cleaning process which is ultrasonic cleaning as follow. In any kind of cleaning with a liquid solvent the process is substantially promoted by application of mechanical stresses; dirt particles which are already partially dissolved will be loosened and eventually torn away as a whole by them.

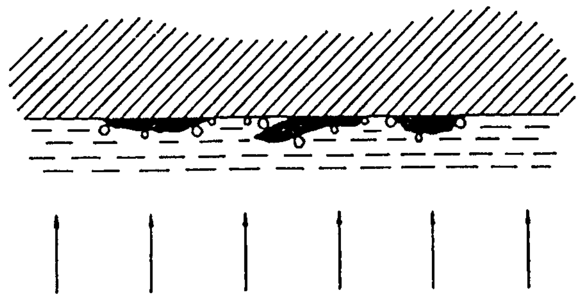

Fig. 2.12 Mechanism for ultrasonic cleaning

The arrows on figure 2.12 show the direction of ultrasonic power's movement. When ultrasonic energy is occurred, this energy will shake the molecule of water to make the quake, when the quake is occurred the clean system is also happened.

It is particularly advantageous for this process that there are always numerous cavitation nuclei on the surface to be cleaned. Therefore, cavitation will occur mainly where it is actually needed. This hold not only for smooth and plane surfaces but also for irregularly shaped surfaces, for parts with impressions or dips of all kinds.

In conventional cleaning these forces are produced by external or internal friction, for instance by treating the contaminated surfaces with brushes, or by squirting them with cleaning solvent. Furthermore, vigorous motion and mixing of the liquid enhances the cleaning process considerably since it continuously removes the used solvent, i.e. that part of it which his already saturated with the contamination, and replaces it with fresh liquid.

And there are also any kinds of cleaning processes by using ultrasonic usefulness which are arrangements of piezoelectric composite transducers for the operation of cleaning as below

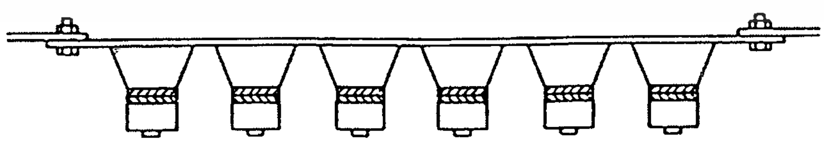

(a)

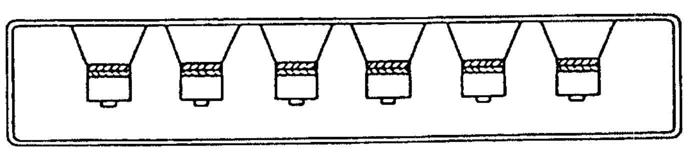

(b)

Fig. 2.13 Arrangements of piezoelectric composite transducers for the operation of cleaning tanks; (a) Removable arrangement, (b) immersion arrangement

Figure 2.13 shows an industrial ultrasound application in cleaning processes. In working of the arrangements of piezoelectric composite transducers for the operation of cleaning tanks; (a) Removable arrangement (figure 2.13(a)), immersion arrangement (figure 2.13(b)).

Chapter 3

Tomographic Processes and Reconstruction Algorithms

The rays of audible sound pass through the object by using some medium which has low diffractive index; the assumption of the non-diffracting source is valid because the refractive index of the traveling path is homogeneous. As a result, the conventional theorem for direct ray can be applied to the computed tomography with a few changes.

Integrations being along straight lines through the object and being referred to as line integrals. We will show that is the key to tomographic imaging

In this chapter, the introduction to the meaning of cross sectional image, tomographic imaging for non-diffracting source, including a parallel-beam tomography and algebraic reconstruction technique, is described concisely.

3.1 Cross-Sectional Image Meaning

In natural, human visible is caused from the incident light at the object. The incident light is reflected to retina of human's eyes and finally displayed on human's eyes as image. Which opaque incident light object will show only the image external surface to human's eyes; not display the internal surface of objects image.

From this limitation, the conventional researcher invented a high electromagnetic energy machine such as X-ray for issuing the object. In the x-ray case, the measured data only approximately correspond to a line integral. The attenuation of an x-ray beam is dependent on the energy of each photon and since the x-rays used for imaging normally contain a range of energies the total attenuation is a more complicated sum of the attenuation at each point along the line. Moreover, there is the other case else; in the ultrasound case; the errors are caused by the fact that sound waves almost never travel through an object in a straight line and thus the measured time corresponds to some unknown curved path through the object. Fortunately, for many important practical applications, approximation of these curved paths by straight lines is acceptable.

Nowadays, fundamental considerations of the projections are used for cross-sectional imaging. There are also the reflection mode and emission tomography beside the existing transmission mode tomography; which each sources will be used in different conditions such as magnetic resonance imaging: MRI or called as nuclear magnetic resonance imaging: NMRI; Magnetic resonance imaging is based on the measurement of radio frequency electromagnetic waves as a spinning nucleus returns to its equilibrium state. Any nucleus with an odd number of particles (protons and neutrons) has a magnetic moment, and, when the atom is placed in a strong magnetic field, the moment of the nucleus tends to line up with the field. If the atom is then excited by another magnetic field it emits a radio frequency signal as the nucleus returns to its equilibrium position. Since the frequency of the signal is dependent on not only the type of atom but also the magnetic fields present, the position and type of each nucleus can be detected by appropriate signal processing.

Both of positron emission tomography: PET and single photon emission tomography: SPECT use a method of gamma-ray photons distribution by injection; a cross section of a body can be shown by a distributed source emitting gamma-ray photons. For the purpose of imaging, any very small, nevertheless macroscopic, element of this source may be considered to be an isotropic source of gamma-rays. Which injecting the gamma-rays to blood vessel causes a body distributed source emitting gamma-ray photons; an emitting quantity is depended on a collection quantity of organs in body. This technique is mostly used for cancer diagnostic because a cancer can be absorbed the gamma-ray photons greater than normal organs. These gamma-ray photons absorptions are depended on the gamma-ray; normally, sugar is mostly used to mix with the gamma-ray photons. Because a high absorption of cancers is caused by higher distribution of gamma-ray photons in those areas than the other then we can notice clearly the position of the cancer.

3.2 Parallel Beam Tomography

When array of sources and array of detectors are arranged correspondingly, the rays are considered as parallel beams since all the rays' paths are parallel to one another. This is the key property of the parallel-beam tomography, the theories of which include parallel-beam projection, Fourier slice theorem, and parallel-beam backprojection.

3.2.1 Parallel Beam Projection Data

Parallel-beam projection, or the *Radon transform*, of function *f(x,y)*, denoted by $P_\theta(t)$, is defined as its line integral along the line AB, which makes perpendicular to another line inclined at angle θ from the *x*-axis, at the distance *t* from the origin. Practically, function *f(x, y)* is the cross-sectional image and function $P_\theta(t)$ is the projection at specific angle.

If the rotated coordinates *(t, s)* from *(x, y)* with angle θ was given by equation 3.1. Then the equation of line AB in Figure 3.1 would become an equation 3.2.

$$\begin{bmatrix} t \\ s \end{bmatrix} = \begin{bmatrix} \cos\theta & \sin\theta \\ -\sin\theta & \cos\theta \end{bmatrix} \begin{bmatrix} x \\ y \end{bmatrix} \qquad 3.1$$

$$x\cos\theta + y\sin\theta = t_1 \qquad 3.2$$

From Figure 3.1, the projection of function *f(x, y)* can be expressed by line integral as the equation 3.3. By changing coordinates to normal and using delta function.

$$P_\theta(t) = \int_{-\infty}^{\infty} f(t,s)ds \qquad 3.3$$

Equation 3.3 is rewritten as equation 3.4 respectively,

$$P_\theta(t) = \int_{-\infty}^{\infty}\int_{-\infty}^{\infty} f(x,y)\delta(x\cos\theta + y\sin\theta - t)dxdy \qquad 3.4$$

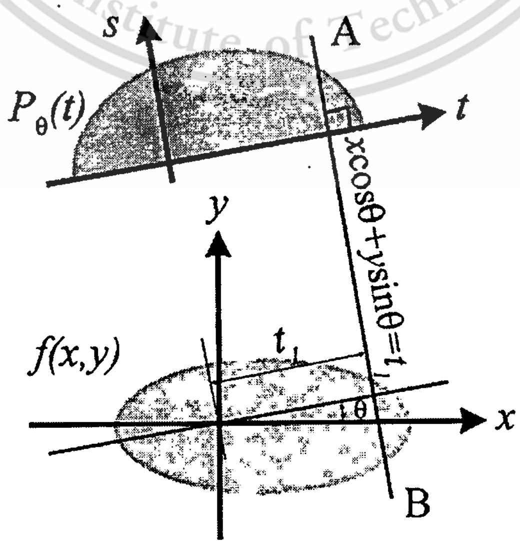

Fig. 3.1 Parallel-beam projection of function *f(x, y)* at angle θ

3.2.2 Fourier Slice Theorem

Figure 3.2 shows proving of the Fourier slice theorem relates one-dimensional Fourier transform of the projection to two-dimensional Fourier transform of the cross-section. This relation is the principle which leads to the filtered-backprojection algorithm. One-dimensional Fourier transform of the projection at angle θ is given by equation 3.5.

Where ω is the frequency axis; substituting equation 3.3 into equation 3.5 yields as follow

$$S_\theta(\omega) = \int_{-\infty}^{\infty} P_\theta(t) e^{-j2\pi\omega t} dt \qquad 3.5$$

$$S_\theta(\omega) = \int_{-\infty}^{\infty} \left[\int_{-\infty}^{\infty} f(t,s) ds \right] e^{-j2\pi\omega t} dt \qquad 3.6$$

Then change the coordinates to *(x, y)* by using equation 3.3 and equation 3.4 becomes an equation 3.7. After that the Two-dimensional Fourier transform of the cross-section can be written as equation 3.8

$$S_\theta(\omega) = \int_{-\infty}^{\infty} \int_{-\infty}^{\infty} f(x,y) e^{-j2\pi\omega(x\cos\theta + y\sin\theta)} dxdy \qquad 3.7$$

$$F(u,v) = \int_{-\infty}^{\infty} \int_{-\infty}^{\infty} f(x,y) e^{-j2\pi(ux+vy)} dxdy \qquad 3.8$$

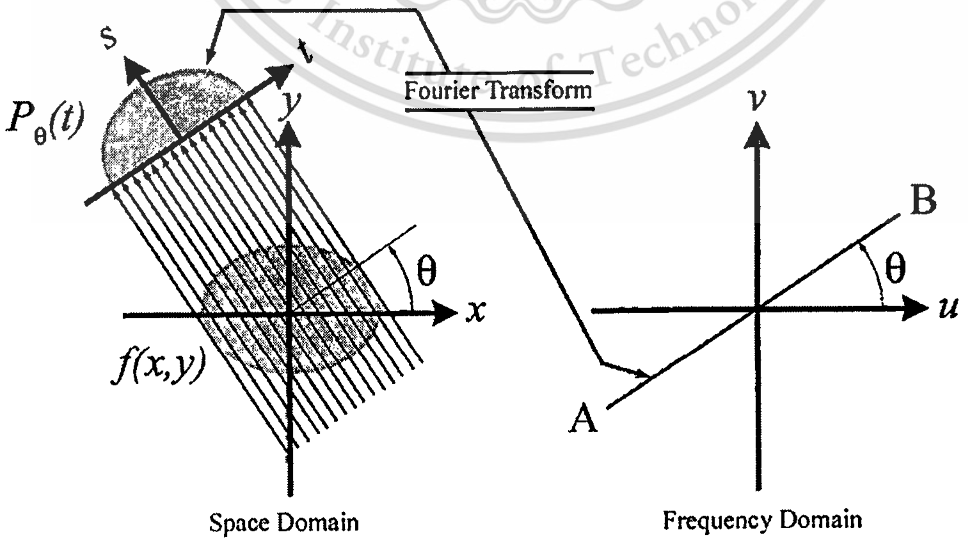

Fig. 3.2 The relationship between the projection of the object and the Fourier transform of the object function

From equation 3.7 and equation 3.8, it is obviously seen that the one-dimensional Fourier transform of the projection $S_\theta(\omega)$ is related to the two-dimensional Fourier transform of the cross section $F(u, v)$ when the polar coordinates (ω,θ) is changed to the Cartesian coordinates (u, v), or

$$S_\theta(\omega) = F(\omega,\theta) = F(\omega\cos\theta,\omega\sin\theta) = F(u,v) \qquad 3.9$$

This relation is the Fourier slice theorem which is stated by [6] as the following:

> The Fourier transform of a parallel projection of an image $f(x, y)$ taken at angle θ gives a slice of the two-dimensional transform, $F(u, v)$, subtending an angle θ with the u-axis. In other words, the Fourier transform of projection data $p_\theta(t)$ gives the value of $F(u, v)$ along line AB in figure 3.2.

3.2.3 Filtered-Backprojection Algorithm

From the Fourier slice theorem, the filtered-backprojection algorithm [20] is derived to reconstruct the cross section from a series of projections. Practically, the backprojection can be thought as smearing all the filtered projections across a 2D-plane as shown in figure 3.3.

Two-dimensional inverse Fourier transform of the $F(u, v)$ is given by

$$f(x,y) = \int_{-\infty}^{\infty}\int_{-\infty}^{\infty} F(u,v)e^{j2\pi(ux+vy)}dudv \qquad 3.10$$

Change from the Cartesian coordinates (u, v) to the polar coordinate (ω,θ) by using

$$u = \omega\cos\theta$$

$$v = \omega\sin\theta \qquad 3.11$$

$$dudv = \omega d\omega d\theta$$

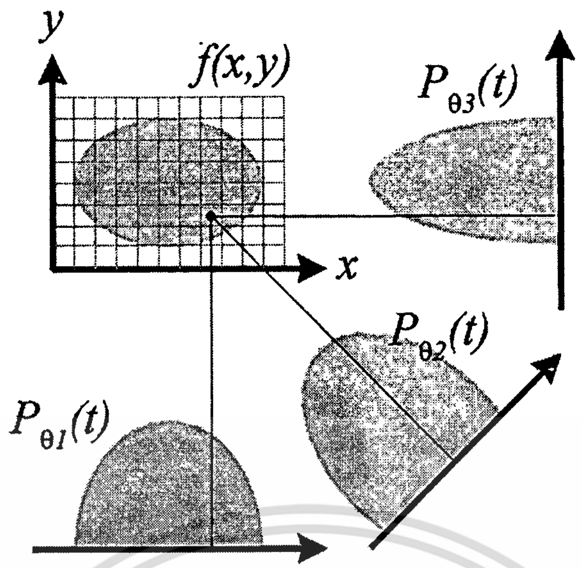

Fig. 3.3 The concept of reconstruction by backprojection

From above equations 3.10 and 3.11, two-dimensional inverse Fourier transform of the $F(\omega,\theta)$ is given by equation 3.12. Then expanding the outermost integration to two parts (equation 3.12), from 0 to π and from π to 2π as equation 3.13

$$f(x,y) = \int_0^{2\pi}\int_0^{\infty} F(\omega,\theta) e^{j2\pi\omega(x\cos\theta + y\sin\theta)} \omega d\omega d\theta \qquad 3.12$$

$$f(x,y) = \int_0^{\pi}\int_0^{\infty} F(\omega,\theta) e^{j2\pi\omega(x\cos\theta + y\sin\theta)} \omega d\omega d\theta$$
$$+ \int_0^{\pi}\int_0^{\infty} F(\omega,\theta+180^\circ) e^{j2\pi\omega[x\cos(\theta+180^\circ) + y\sin(\theta+180^\circ)]} \omega d\omega d\theta \qquad 3.13$$

Using property in equation 3.14 to equation 3.13 then we can rewrite as equation 3.15

$$F(\omega,\theta+180^\circ) = F(-\omega,\theta) \qquad 3.14$$

$$f(x,y) = \int_0^{\pi}\int_{-\infty}^{\infty} F(\omega,\theta) e^{j2\pi\omega t} |\omega| d\omega d\theta \qquad 3.15$$

From the Fourier slice theorem in equation 3.9; the projections are related with the cross section by this expression

$$f(x,y) = \int_{0}^{\pi}\int_{-\infty}^{\infty} S_\theta(\omega)|\omega| e^{j2\pi\omega t} d\omega d\theta \qquad 3.16$$

An equation 3.16 is the filtered-backprojection algorithm, in which $|\omega|$ is the ramp filter and *so (ω)* is the Fourier transformation of the projection $P_\theta(t)$. The algorithm can be separated into two parts; the backprojection and the filtration, as equation 3.17 and equation 3.18

$$f(x,y) = \int_{0}^{\pi} Q_\theta(x\cos\theta + y\sin\theta) d\theta \qquad 3.17$$

$$Q_\theta(t) = \int_{-\infty}^{\infty} S_\theta(\omega)|\omega| e^{j2\pi\omega t} d\omega \qquad 3.18$$

3.3 Ultrasonic Computed Tomography

Ultrasound computed tomography (UCT) is very similar to x-ray tomography. In both cases a transmitter illuminates the object and a line integral of the attenuation can be estimated by measuring the energy on the far side of the object. Ultrasound differs from x-rays because the propagation speed is much lower and thus it is possible to measure the exact pressure of the ultrasonic wave as a function of time. From the pressure waveform it is possible, for example, to measure not only the attenuation of the pressure field but also the delay in the signal induced by the object. From these two measurements it is possible to estimate the attenuation coefficient and the refractive index of the object.

Ultrasonic computed tomography (UCT) can be classified into two mode. Those are transmission-mode UCT and reflection-mode UCT. The first one will be discussed in section 3.4.1 and the other one will be discussed in section 3.4.2.

3.3.1 Fundamental Transmission-Mode UCT

Transmission-mode UCT like the x-ray case, first consider ultrasonic waves propagating from a transmitting transducer through a single layer of tissue and measured by a receiver on the far side of the tissue, as diagram in figure 3.4.

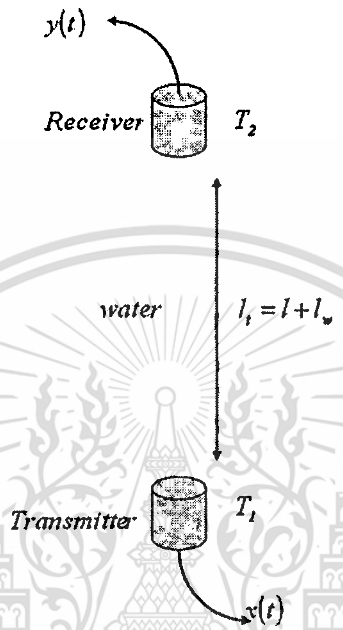

Fig. 3.4 the beam undergoes a phase shift as it goes through the water

Figure 3.4 shows as an ultrasonic beam travels between two transducers in the case of the beam undergoes a phase shift as it goes through the water which has an internal intensity value which shown equation 3.19

$$Y_w(f) = X(f)H_1(f)H_2(f)\exp[-[\alpha_w(f) + j\beta_w(f)](\ell + \ell_w)] \qquad 3.19$$

Where

$Y_w(f)$	is the Fourier transform of $y_w(t)$
$X(f)$	is the Fourier transform of $x(t)$
$H_1(f)$	is the transfer function of the transmitter
$H_2(f)$	is the transfer function of the receiver
α_w	is the frequency-dependent attenuation coefficient of the water.
β_w	is the frequency-dependent phase coefficient of water.

In addition, because ultrasonic waves in the range 1 to 10 MHz are highly attenuated by air, the tissue layer is immersed in water or another fluid. Water serves to couple the energy of the transducer into the object and provides a good refractive index match with the tissue. Ignoring the effects of refraction, here we will model the received waveform by considering only the direct path (or ray) between the two transducers.

Furthermore, the related equation of this figure can be shown as equation 3.19 where a received signal is directly related to a transmitted signal, the transfer function of transmitter and receiver especially related to the attenuation of ultrasound in water.

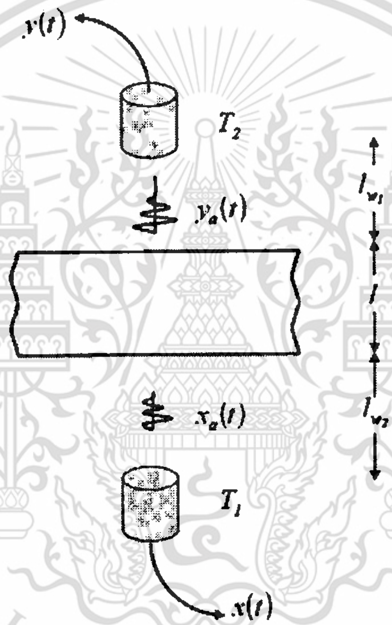

Fig. 3.5 As an ultrasonic beam travels between two transducers through water and object.

Figure 3.5 shows as an ultrasonic beam travels between two transducers in the case of the beam undergoes a phase shift as it goes through the water which has an internal intensity value which shown equation 3.20.

The related equation of this figure can be shown as equation 3.20 where an ultrasonic beam travels between two transducers through water and object; where a received signal is directly related to a transmitted signal, the transfer function of transmitter and receiver especially related to the attenuation of ultrasound in water.

$$Y(f) = X(f)H_1(f)H_2(f)A_\tau$$
$$.\exp[-[\alpha(f) + j\beta(f)\ell]\exp[-[\alpha_w(f) + j\beta_w(f)]\ell_w] \qquad 3.20$$

Where

$Y(f)$ is the Fourier transform of over all of medium $y(t)$

A_τ are the transmittances of the front and the back faces of the layer. ($A_\tau = \tau_1.\tau_2$)

$\alpha(f)$ is the attenuation coefficient of the tissue layer

$\beta(f)$ is the phase coefficient of the tissue layer

ℓ is the thickness of the object

ℓ_w is the water path lengths on two sides of tissue layer ($\ell_w = \ell_{w1} + \ell_{w2}$)

Now we mention about the using re a relationship of equation 3.19 and equation 3.20 then we can rewrite as equation 3.21

$$Y(f) = Y_w(f)A_\tau \exp[-[(\alpha(f) - \alpha_w(f))\ell + j(\beta(f) - \beta_w(f))\ell]] \qquad 3.21$$

When we consider the ultrasonic attenuation for the water medium $\alpha_w(f)$ from (table A.1 in appendix A) the ultrasonic attenuation for the water medium $\alpha_w(f)$ is much smaller than the ultrasonic attenuation for the tissue medium and the ultrasonic attenuation for the water medium may simply be neglected.

$$Y(f) = Y_w(f)A_\tau \exp[-[(\alpha(f) + j(\beta(f) - \beta_w(f))\ell]] \qquad 3.22$$

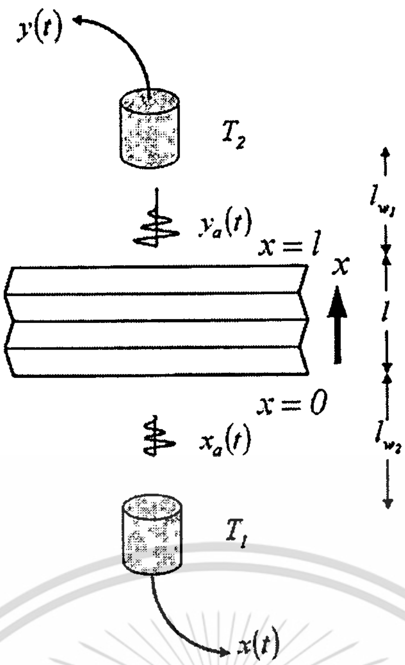

Fig. 3.6 As an ultrasonic beam travels through both the water and a multilayered object.

Extending this rationale to multilayered objects such as the one shown in figure 3.6, we get for the Fourier transform *Y(f)* of the received signal:

$$Y(f) = X(f)H_1(f)H_2(f)A_\tau \exp\left[-\int_0^\ell [\alpha(x,f) + j\beta(x,f)]dx\right] .\exp[-j\beta_w(f)\ell_w] \qquad 3.23$$

Where

$\alpha(x, f)$ is the attenuation coefficient of the tissue layer at x

$\beta(x, f)$ is the phase coefficient of the tissue layer at x

Now, they are functions of position along the path of propagation.

An equation expresses the relation between an ultrasonic beam travels through the water and a multilayered object can be shown as equation 3.24.

Where a received signal is directly related to a transmitted signal, the transfer function of transmitter and receiver especially related to the attenuation of ultrasound in water. In addition, the attenuation of ultrasound is depended on the specific medium that ultrasound has passed.

Equation 3.23, we may consider size effect depended on attenuation and phase-shifted effect depended on phase changing. Using a relation between equation 3.24 and equation 3.25 then we can rewrite as equation 3.26,

$$\beta(x,f) = 2\pi f / V(x) \qquad 3.24$$

$$\beta_w(f) = 2\pi f / V_w \qquad 3.25$$

$$Y(f) = A_{\tau} Y_w(f) \exp[-\int_0^{\ell} \alpha(x,f)dx] \cdot \exp[-j2\pi f \int_0^{\ell} (1/V(x) - 1/V_w)dx] \qquad 3.26$$

Where

$V(x)$ is propagation velocity in the layer at x

V_w is propagation velocity in the water

Equation 3.26, we may consider $y(t) = y'_w(t - t_d)$ to be an "attenuated" water path signal. This is the assumed signal that would be received if it underwent the same loss as the actual signal going through tissue. By the shift property, the relationship depicted in equation 3.26 may be expressed as

$$T_d = \int_0^{\ell} \left(\frac{1}{V(x)} - \frac{1}{V_w}\right) dx \qquad 3.27$$

In equation 3.27, we can imply our discussion on refraction; a comparison of actual signal goes through tissue and water in equation 3.28 can be rewritten as

$$n(x) = \frac{V_w}{V(x)} \qquad 3.28$$

$$T_d = \frac{1}{V_w} \int_0^{\ell} (1 - n(x)) dx \qquad 3.29$$

In equation 3.27 and 3.29 shows the time data during an ultrasonic pulse wave's traveling passed through tissue. These projections data are used to reconstruct the cross-sectional object which called as "sound velocity tomography."

In addition, if we adjust an existing sound velocity data of equation 3.15 to be refractive index data we will call this tomography as the "refractive index tomography." which shown as equation 3.30 will be discussed next section.

3.3.2 Projection Data Estimation for Transmission-Mode UCT

The refractive index of the object calculation method is depended on delay time during ultrasonic pulse wave travels. The differences between delay time of ultrasonic pulse wave travels of water path and object path in one round of linear scan.

Ultrasonic Refractive Index Tomography on Transmission-Mode UCT: is related to the phase shift and the attenuation of an ultrasonic signal, *x(t)*, as it travels through water, $y_w(t)$, and is attenuated, $\dot{y}_w(t)$, and then phase shifted by the object, *y(t)*, are shown on figure 3.7. The diffractive index of water is related to water used to compare sound velocity while neither there is object nor there is not object. When we considerate the equation 3.30, we will see the object diffractive index estimation.

$$n_o = \frac{v_o}{v_w} \qquad 3.30$$

When

n_o denotes for the refractive index of object

v_o denotes for the object sound velocity

v_w denotes for the sound velocity in water, normally it contains 1500 m/s sound velocity

from the equation 3.31, we saw that it does not express a sound velocity. But the sound velocity in water at any temperature is always expressed.

$$v = \frac{l}{t} \qquad 3.31$$

When

l represents to the total path length at time t

t represents to the time at distance l

Suppose that, we replace the sound velocity as equation 3.32 into equation 3.33. Then we can rewrite them as below.

$$n_o = \frac{v_o}{v_w} = \frac{l_o / t_o}{l_w / t_w} \tag{3.32}$$

Equation 3.32 shows a consideration of water path length (l_w) and object path length (l_o); which water path length is equal to object path length or ($l_o = l_w$) then give us a results of a period that ultrasound used for traveling. We can use the ultrasonic traveling period to find the diffractive index shown as equation 3.34

$$n_o = \frac{t_w}{t_o} \tag{3.33}$$

The diffractive index equation is shown as equation 3.33 is used to find the diffractive index in our experiment. In addition, the measured signals are achieved from oscilloscope can give us only the data in time domain (delay-timed data). Furthermore, equation 3.33 is the diffractive index solution which gives us directly the position of ultrasound. On that equation, we can use the time of ultrasound's traveling to find the diffractive index.

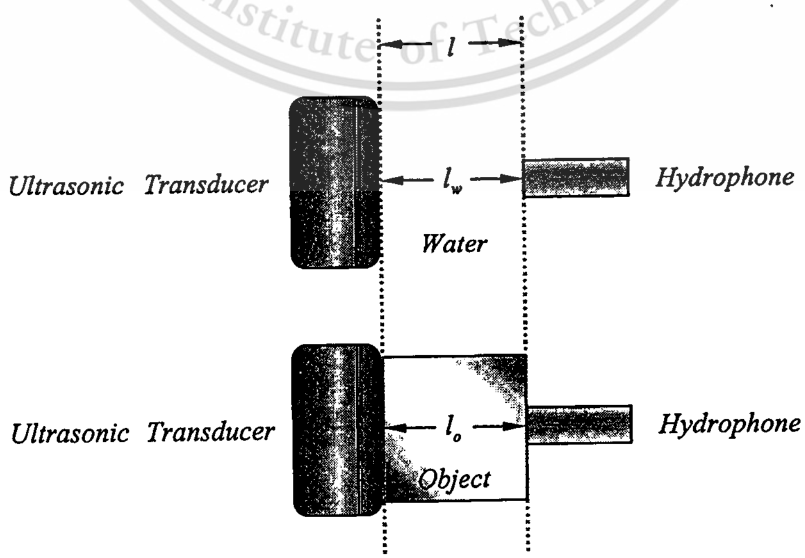

Fig. 3.7 Basic schematic model of object diffractive index estimation

Figure 3.7 shows a signal. An ultrasound passes through the same distance in different time. The time of ultrasound's traveling is depended on the object density where area has high density object can absorb more ultrasound as well then give us more time consumption of ultrasonic's traveling in water.

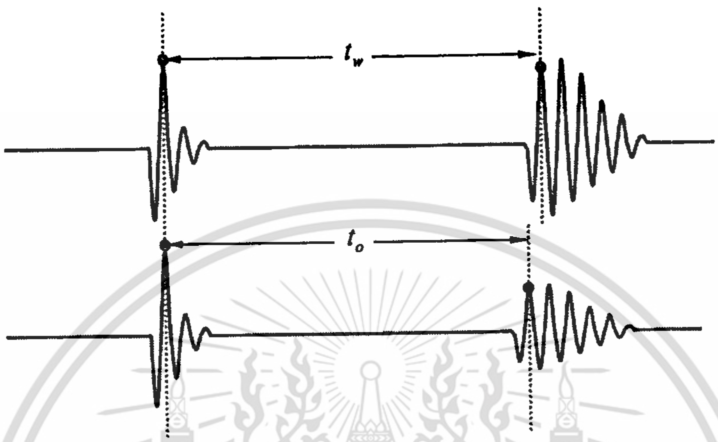

Fig. 3.8 A graph of calculation of the time of the ultrasound; above model represents a water path length signal while a bottom model represents an object path length signal.

This limitation of the ultrasonic diffractive index tomography is the diffractive index measurement. The phantom model must be measured before scanning by ultrasonic transducer. This technique can measure only the specific objects that connected to a transducer. The specific objects should be only the rectangular shape that invented by the mould.

The diffractive index of phantom will not be measured in necessary value, if there is an interior gap or other density in specific phantoms.

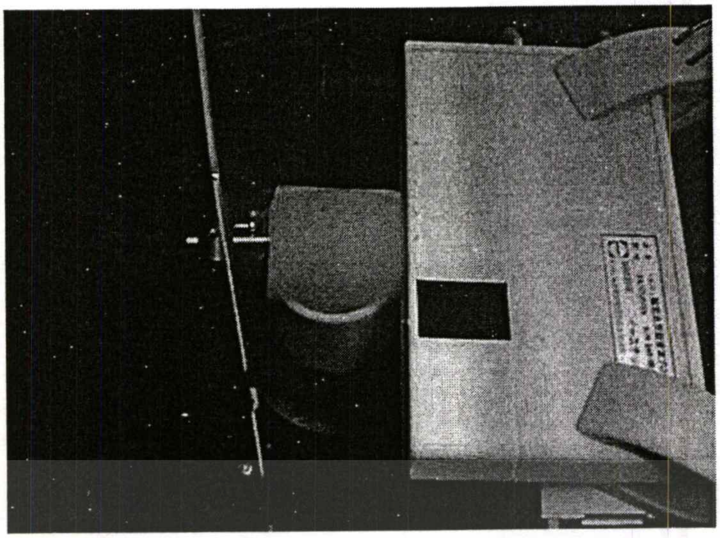

Fig. 3.9 A rectangular homogenous phantom diffractive index measurement

Figure 3.9 shows a rectangular homogenous phantom is measured a refractive index by a refractive index measurement.

Practical Concept of Projection Data Estimation for Transmission-Mode

A procedure of projection data estimation for transmission-mode UCT [8] is used to calculate the object projections at specific angles (i.e. 2, 4, 6, 10 degree angle interval). In the procedure of collecting the projections, the objects were issued on parallel linear scan direction. In addition, the obtained specific signals are displayed on the oscilloscope can be shown as figure 3.13. In addition, the obtained projections at each scanning point are transmitted to the PC by using a GPIB card.

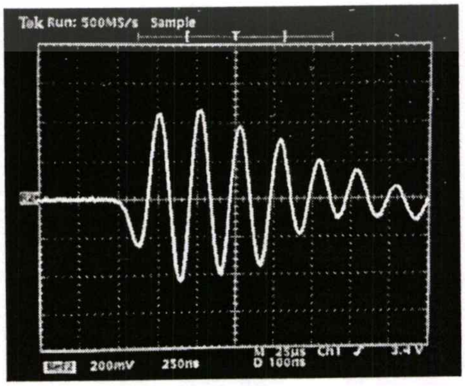

Fig. 3.10 A obtained signals is recorded on an oscilloscope

In addition, of a procedure of projection data estimation for transmission-mode UCT [8]; here our aim is making the cross-sectional images from the refractive index coefficient of soft tissue projections where the acquisition system can be shown as figure 3.11.

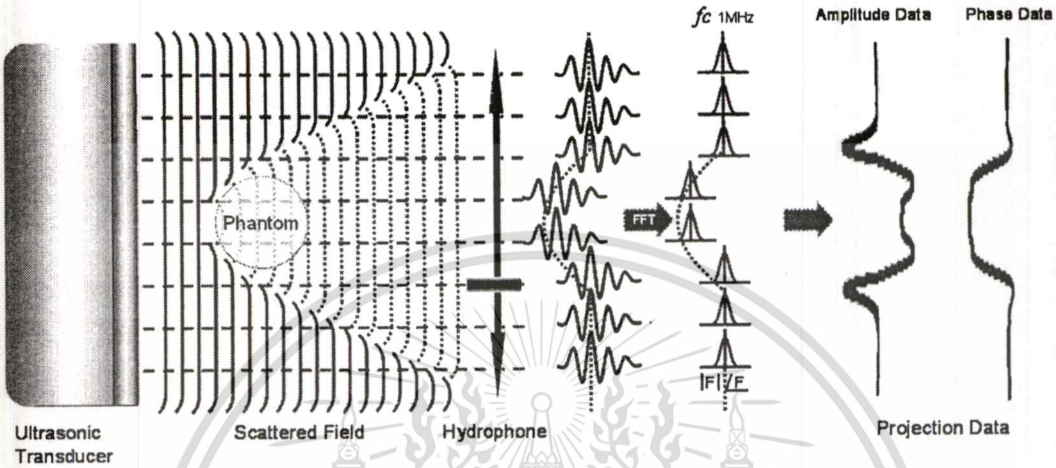

Fig. 3.11 A schematic of projections estimation from delay time in transmission-mode UCT

In the transmission-mode UCT [8], ultrasound image sequence transmission experiment was performed using 3.5MHz ultrasound frequency to evaluate this system. The experiment showed projection data results. Resolution preference method enables to display an ultrasound image in the resolution of 128 x 128 pixels of the image. Furthermore transmission delay [8] was less than 1 second in this method. This system is expected to be useful for breast cancer diagnostic basis having high resolution and frame rate.

Transmission- mode Ultrasonic Tomographic System

The transmission-mode UCT system can be expressed as the acquisition figure 3.12. The system consists of a 3.5MHz ultrasonic transducer and the wide-band ultrasonic hydrophone submerged in the water tank lining with anti-reflective material. The transducer and the hydrophone are connected to a computer-controlled linear scanning system which is capable of moving 1mm/step. In the transmission mode UCT, similar to the x-ray CT,

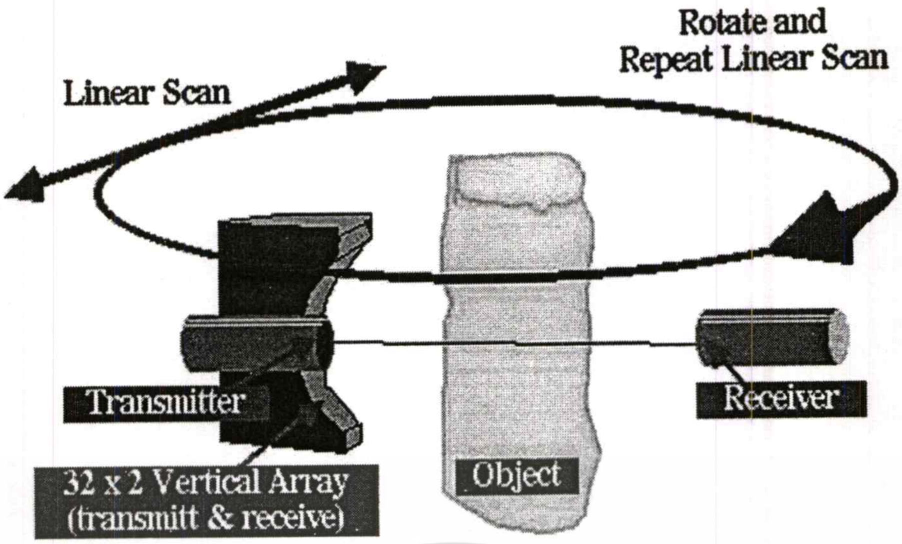

Fig. 3.12 Basic schematic of transmission-mode ultrasonic tomography

the transducer and the hydrophone are aligned on the opposite site of the phantom. In each position, the integrated refractive index of the phantom, i.e. the projection data, is measured from the difference between the transit time of ultrasound through the phantom and the transit time through the direct water path. After completing linear scan, the phantom is rotated and a projection collection process is repeated.

3.3.3 Fundamental Reflection-Mode UCT

In this thesis, we aim into the reflection-mode tomography. The basic aim of reflection-mode UCT is to construct a quantitative cross-sectional image from reflective data. One nice aspect of this form of imaging, especially in comparison with transmission tomography, is that it is not necessary to encircle the object with transmitters and receivers for gathering the "projection" data; transmission and reception are now done from the same side.

Projections data estimation, this thesis focuses on frequency-shifted method to estimate the projection data by using the shifting of power spectrum.

Finding the projections from the frequency-shifted method [23-24] is the algorithm used for projection estimating the projections data. The procedure is used in calculating the projections data from the attenuation coefficient values shown as figure 3.14.

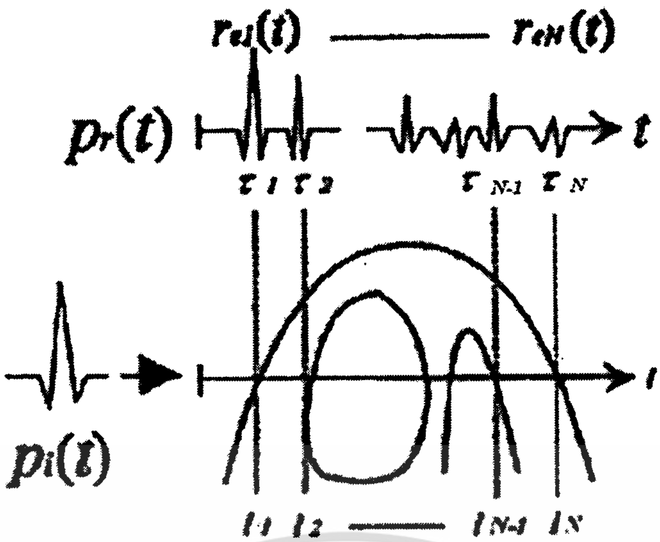

Fig. 3.13 The waveform of incident and reflected pulse. Where the reflections occur at the tissue interfaces.

Figure 3.13 shows the principle of the reflection-mode ultrasonic tomography. when the tissues is issued by an incident ultrasonic pulse wave then the ultrasonic pulse wave will pass a multilayer of the tested tissue next give us reflected ultrasonic pulse wave but in this method integrated linear slope we focused on the only the latest ultrasonic pulse wave which issued the last layer of the object.

Firstly, the basic principle of reflection mode UCT mentioned; the above mathematical procedure illustrates an ultrasonic computed tomography in reflection mode which contains transmitted/received signals on the same transducer. A collection of the projection data can be obtained from the attenuation coefficient values while the attenuation coefficient $\alpha(x, y)$ is then able to be computed from the differences of logarithm of power spectrums of the incident pulses and the reflected pulses because $\alpha(x, y)$ is the distribution of the spectrum analysis of the attenuation coefficients.

Figure 3.13; the object is insonified by a pulse beam wave $p_r(t)$ and a reflected signal $p_r(t, X : \theta)$, where θ is a function of the insonifying angle and t is time; both of these signals are measured on the same transducer. This system in figure 3.13 is roughly the same as the pulse-echo ultrasonic imaging system. Therefore, technology transfer from the conventional system is easy. Also, figure 3.13 proves that is possible to measure the data even though there is bone together with a scanning line.

Secondly, we mentioned about the projection data estimation which derived from extracting integrated attenuation coefficient from the reflected ultrasonic pulse wave which assumed as the linear frequency independent model of the attenuation coefficient; this method will be known as the process of proposed method shown in figure 3.14.

Bring to mind again that $p_r(t, X : \theta)$, or simple $p_r(t)$, is a time-varying signal which consists of pulses reflected at tissue-tissue and object-water interfaces as exposed in figure 3.13. The transmittance and the reflectance at the n^{th} interface; then, considering that the attenuation coefficient is proportionate to frequency under the assumptions that ultrasound travels in straight lines through the media and that the attenuation of absorption is the only attenuation, $p_r(t)$ is expressed as

$$p_r(t) = \sum_{n=1}^{N} r_{en}(t) \qquad 3.34$$

$$r_{en}(t) = \sum_{n=1}^{N} r_{n,n+1}\left(\prod_{k=1}^{n-1} t_{k,k+1} \cdot t_{k+1,k}\right) x\, p_i\left(t-\tau_n\right) e^{-2\int_{l_1}^{l_n} \alpha(x,y).f dY} + n(t),$$

$$r_{en}(t) = \sum_{n=1}^{N} \sqrt{R}_N \left(\prod_{k=1}^{n-1} T_k\right) x\, p_i\left(t-\tau_n\right) e^{-2\int_{l_1}^{l_n} \alpha(x,y).f dY} + n(t) \qquad 3.35$$

Where N is the number of tissue-tissue and object-water interfaces, τ_n is the delay time matching with the distance from the transducer to the n^{th} interface, f is frequency, $n(t)$ is white noise and $\alpha(x,y)$ is the distribution of the slope of the attenuation coefficient.

Here, recall that $p_r(t)$ has its bandwidth in the frequency domain. In this equation, we record the last echo pulse, $r_{en}(t)$. Then, by the temporal Fourier transform, equation 3.36 is shown as

$$R_{eN}(f)=\sqrt{R_N}\left(\prod_{K=1}^{N-1}T_K\right)\times P_i(f)\times e^{-2\int_{l_1}^{l_N}\alpha(x,y,f)dl}\times e^{-2\int_{l_1}^{l_N}\beta(f)dl} \qquad 3.36$$

Where $R_{eN}(f)$, $P_i(f)$ is the temporal Fourier transform of $r_{en}(t)$ and $p_i(t)$. This equation demonstrates for that the center frequency of $R_{eN}(f)$ is shifted to a low frequency than that of $P_i(f)$. As a result, the waveform of $r_{en}(t)$ happens to be slower than that of $p_i(t)$ since the higher the frequency is, the larger the value of the attenuation coefficient is. Where $\beta(f)$ is the phase shift of the tissue.

The frequency shifting method firstly purposed for the reflection mode tomography. It is employed to extract the integrated attenuation coefficient from the reflected waveform, as shown in equation 3.37. This method assumes the linear frequency dependent model of the attenuation coefficient, or $\alpha(f) = \alpha 0|f|$.

$$\int_{ray}\alpha_0(x,y)ds=\frac{f_0-f_r}{\sigma^2} \qquad 3.37$$

The value f_0 and f_r are the frequency where the amplitude of the incident pulse and the latest reflected pulse are maximum value, and σ^2 is the variance of the power spectrum. In the case of reflection mode, half must be divided from the right hand side of the formula by the fact that the received pulse travel forth and back through the tissue. The flowchart of this method can be show as figure 3.14.

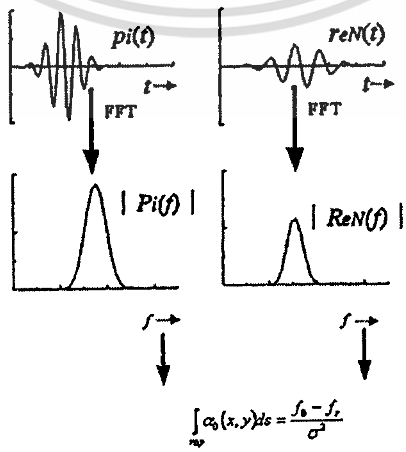

Fig. 3.14 The processes of deriving the projection data

Figure 3.14 is the processes of deriving the projections data. This process shows how to find the projections data from calculating the attenuation by using the frequency-shifted method. An estimation of the projections data from the frequency-shifted method is the way to extract the projection data by the different peaks of the first incident ultrasonic pulse wave $p_i(t)$ and the latest reflected ultrasonic pulse wave $r_{en}(t)$. Firstly, we take Fourier transform of the first incident ultrasonic pulse wave $P_i(f)$ and the latest ultrasonic pulse wave $R_{eN}(f)$ to find the power spectrum. The power spectrums give us the peak of the incident ultrasonic pulse wave and the latest reflective ultrasonic pulse wave. Finally, we can calculate the different peaks values between the incident ultrasonic pulse wave and the latest reflective ultrasonic pulse wave as shown in figure 3.14 then the results give us a value that related to a projection data.

To provide numerical evidence, we opt to use the Mean Square Error (MSE) for deriving the error between the reconstructed image and the original image. The formula of MSE is given by equation 3.38

$$MSE = \frac{\int \int [o(x,y) - o'(x,y) -]^2 \, dxdy}{\int \int [o(x,y)]^2 \, dxdy} \times 100 \qquad 3.38$$

In equation 3.38, the mean square error can be calculated from the integral 2D data of the original object and the reconstructed object with power 2 then divided by the integral 2D data of the original object, final MSE results (the error results) give us in percentage error by multiplying the 100 percent.

The object attenuation coefficient value is mainly calculated for deriving the projection data in reflection-mode UCT.

This thesis introduces the attenuation coefficients estimations in a way of the frequency-shifted methods which is discussed as followed.

Using the referred table A.2 (appendix A) is expressed about the ultrasonic attenuation in specific medium such as soft tissue. We then can find the object thickness. In object thickness measurement can be done by the sound velocities and sound distances passed through the objects shown as below equation 3.39

$$S = v \, x \, t \qquad 3.39$$

Where

S is the ultrasonic traveling path length (m).

v is the ultrasonic velocity passed through the water (m/s).

t is the pulse period.

The above equation can be applied to calculate the reflected pulse position.

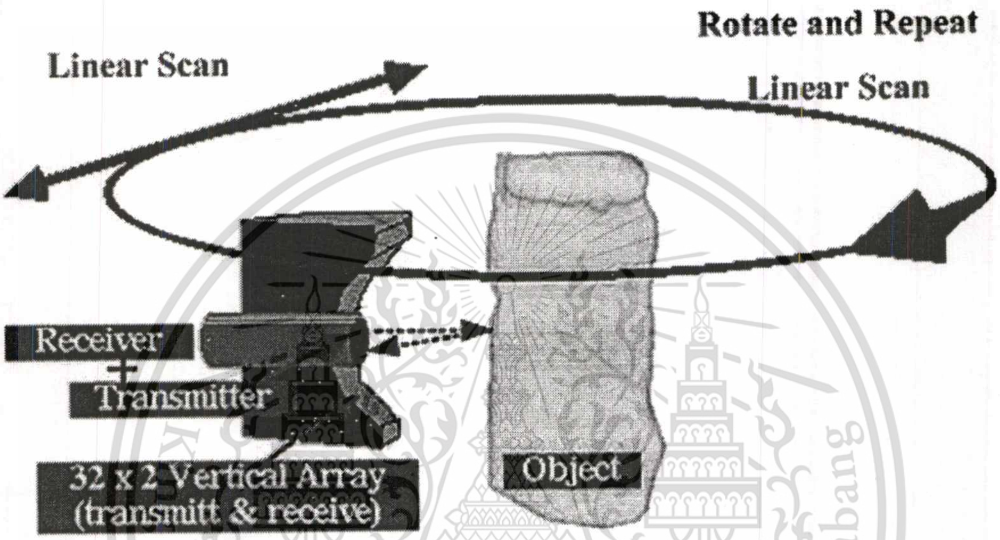

Fig. 3.15 Basic schematic of reflection-mode UCT

Reflection-mode Ultrasonic Computed Tomographic system

Reflection mode UCT shown as figure 3.15 is the system that used for investigating where the transmission and reception are now done from the same side and also submerged in the water tank lining with anti-reflective material. The ultrasonic transducer is connected to a computer-controlled linear scanning system which is capable of moving 1mm/step. In the reflection mode UCT, similar to the x-ray CT, the ultrasonic transducer is aligned on the opposite site of the phantom. After completing linear scan, the phantom is rotated and a projection collection process is repeated. From these two measurements it is possible to estimate the refractive index and the attenuation coefficient of the object.

Chapter 4

Experiments and its Results

An introduction about the reflection-mode UCT with integrated linear slop and frequency-shifted method was applied and practiced in chapter 3 is a basic principle for the real simulation and experiment that will be introduced and expressed in this chapter. This chapter mentions about the simulated system and experimental system including their reconstructed results on various tested models and objects. In addition, the chapter will be systematically organized as listed follow: (i) simulated system, its results, (ii) experimental system, ultrasonic transducer (reflection mode), pulse generator (Pulser), water tank, translator + rotating platform, oscilloscope, personal computer, projection estimation from obtained data, reconstructed results.

4.1 Experimental System

The experimental system is a system that is used to collect the projections data from various objects such as: metals (a cylinder metal, a non-cylinder), phantom (homogenous, in-homogenous). The experimental system operation can be demonstrated as following: the 5MHz ultrasonic pulse is generated from pulse generator to a transducer. The generated pulse will be transmitted to the test objects (called phantoms) and reflected from them; the test objects must be submerged in the water tank with around 30cm high + 60cm length to avoid a multi-reflection case. The medium for this experiment is the water. Because the ultrasonic signal has a bit changes (0.0025 dB/cm referred from table 3.1) in water. The transducer is mounted on the cylinder aluminum which attached to motors. It will be translated 1 mm step by motor controlling. The transducer will be translated from left-to-right (or right-to-left) till projections data are achieved in sufficient views.

Signal-to-Noise Ratios (SNR), the Signal-to-Noise ratios in experimental system are ignored because the ready phantom (tested object) used in the experiment. The tested objects are symmetry and homogenous properties.

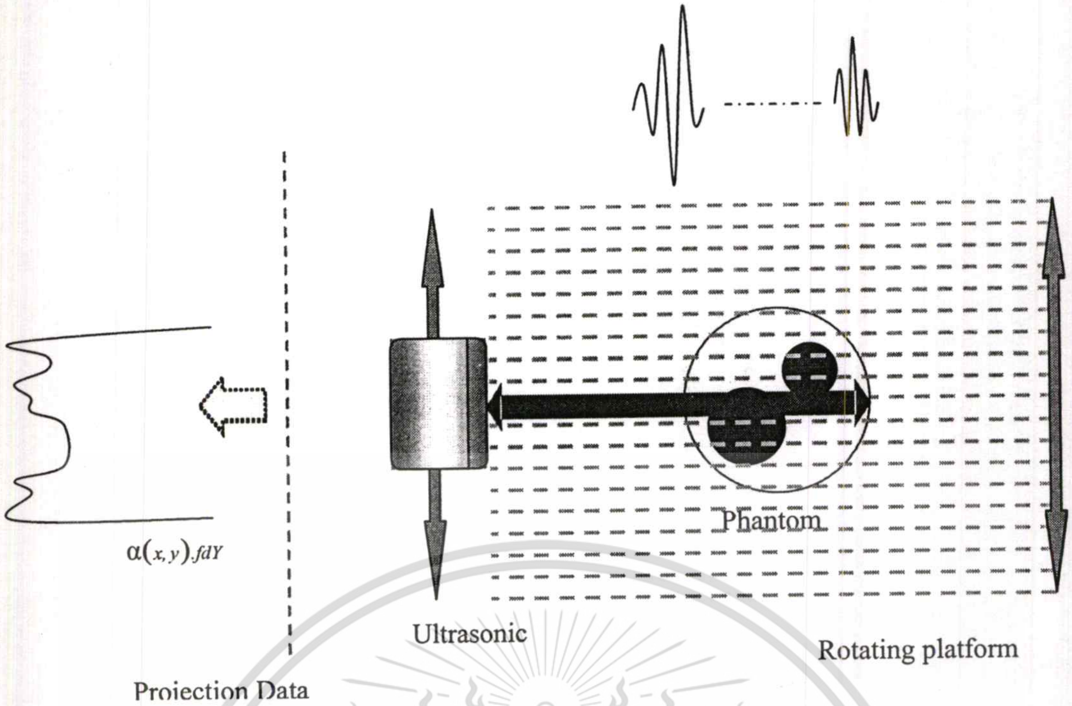

Fig. 4.1 A schematic of an acquisition system

The obtained projections data from each view of linear scans are recorded by personal computer (whenever obtaining the every one projection data along one linear scan is achieved) by using a GPIB card interface worked as a connector to the PC. After altogether sufficient view along linear scan line are completed. We then take those of projections data in sufficient views to reconstruction algorithms such as: simple backprojection and/or filtered backprojection for reconstructing the cross-sectional image/object results.

Note that, the rotating platform will be rotated whenever one projection data is achieved. It is rotated to allow the ultrasonic transducer to scan in other angles till finishing altogether projections data; the rotating platform will be controlled by adjusting angle toll while the adjusting angle tool will be again controlled by user.

In addition, the components of the experimental system can be listed as following: an ultrasonic transducer, an ultrasonic impulse generator, a water tank, a translator part and rotating platform. All detail and model for those components can be introduced as the next section.

4.1.1 Ultrasonic Transducer

Ultrasonic transducer is a main component in our experimental system which used to scan and receive the data from insonifying the object.

V309-SU-F

Fig. 4.2 Ultrasonic transducer used in experimental system

An ultrasonic transducer (figure 4.2) is used in system works as a plane-wave function with resonance frequency at 5MHz. it will transmit every 5MHz to the test object and reflects whenever it sees the different diffractive index of tissue; it transmits/reflects 5MHz ultrasonic frequency, but the frequency shifting is occurred because of the attenuation of the ultrasound after reflecting occurred.

The cylinder transducer can scan in a wide length of linear scan and saving a time for scanning. In addition, the advantage of this ultrasonic transducer can be listed as: the immersion technique provides a means of uniform coupling; Quarter wavelength matching layer increases sound energy output.

4.1.2 Ultrasonic Impulse Generator

Ultrasonic impulse generator works as generating the ultrasonic impulse for ultrasonic transducer. An Ultrasonic Impulse Generator is manufactured by Panametrics Company Limited.

The ultrasonic impulse generator also works in two mode; the transmission-mode and the reflection-mode.

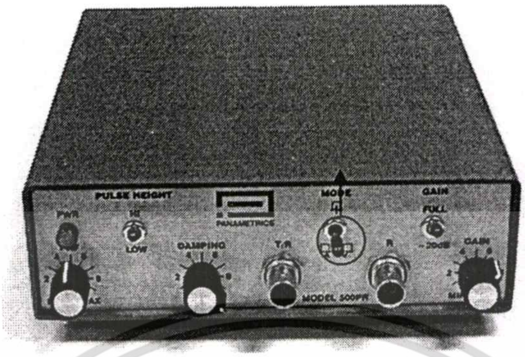

Fig. 4.3 Ultrasonic Impulse Generator, Panametrics Model : 500PR

4.1.3 A Water Tank

This water tank is used for containing the medium water, sized as 35cm high x 70 cm length area. It is not used for containing the medium water but it is also used for allowing other experimental equipments such as: translator part, rotating platform, and etc, shown as below figures 4.4 and 4.5. As noticing at the water tank's wall, we can see signals absorber components attached around it for defending multi-reflection of ultrasound. Ultrasonic test systems can take several forms, but the most common for automated test is immersion testing. To have good acoustical impedance matching between the couplet and the UUT and free range over the entire surface of the UUT, many test systems use an immersion tank filled with water.

4.1.4 Translator Part and Rotating Platform

This stage consists two parts: a translator stage that is controlled by step motor to translate a translator stage step by step on projections collection procedure while a rotating platform is controlled by user. It will support a rotation of objects for adjusting angles by a user whenever a collecting the projections data are achieved at a time of linear scanning. A rotating platform can be shown as figure 4.4.

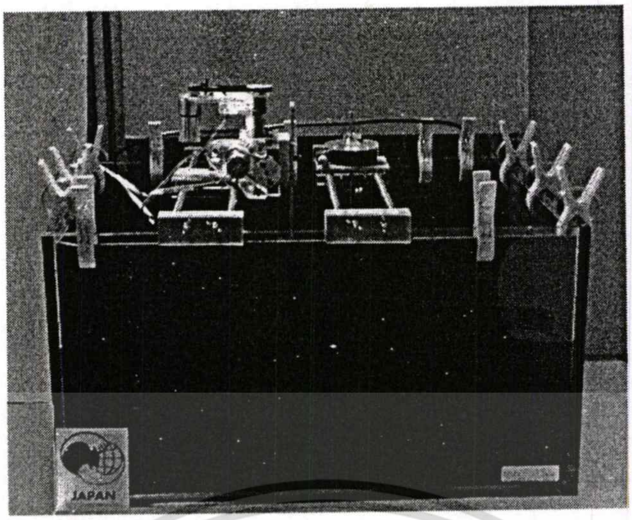

(a) Side View

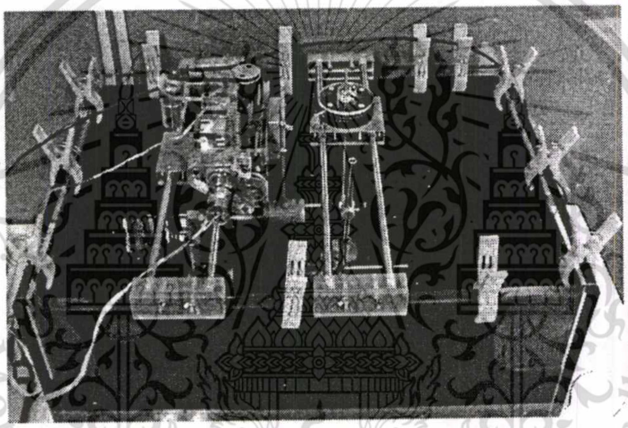

(b) Over View

Fig. 4.4 A water tank in our experimental system

4.1.5 Oscilloscope

An oscilloscope is mainly component in our experimental system. It works as a function of monitoring the signals such as: a trigger signal (shown as channel 2), received signal (shown as channel 1). After monitoring the signal, scope will transmits the obtained signals to the personal computer which connected by GPIB card works as connecter between pc and scope.

Recall, the oscilloscope is used for transmitting the data to personal computer for procession besides measurement and records any signals. In this experimental system a Tektronix

Model: TDS 360 oscilloscope, a GPIB card (IEEE-488 GPIB: General Purpose Interface Bus) is used for displaying the signals and being medium between transferring the signal to the PC.

In any period, a 1000 points ultrasonic pulse signal is transmitted to the PC sampled by high sampling frequency (at 25MHz) which the obtained data has probability as 256 values and transmitted as 8 bit ASCII which are 0x00 till 0xFF.

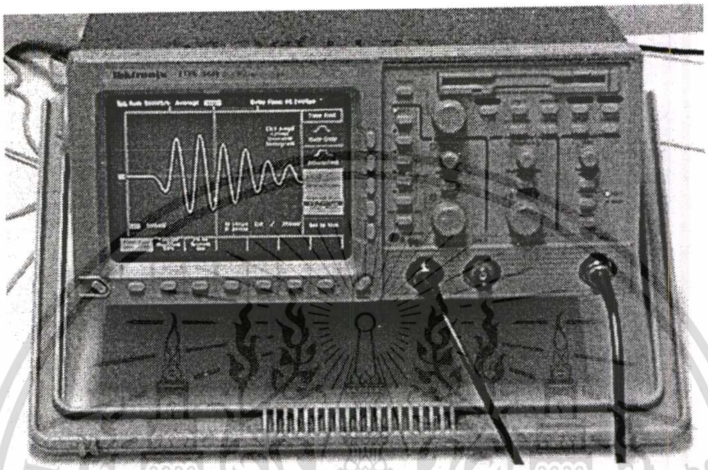

Fig. 4.5 An oscilloscope is used in our experimental system

The oscilloscope's operation; in an ultrasonic pulse measurement is mainly read as wide length time axis so it reason that an oscilloscope give us a data in period. The general measurement of the oscilloscope is in period of time. So the users can adjust a time bottom to display any period of the displayed pulses.

4.1.6 Personal Computer (PC)

One main important in this experimental system is a Personal Computer (PC) used for signals processing including the receiving the signals form oscilloscope. The PC's components are as listed follow: central processing unit: CPU Intel® Pentium3 733 MHz, with Random access memory: RAM 512 MB memory size.

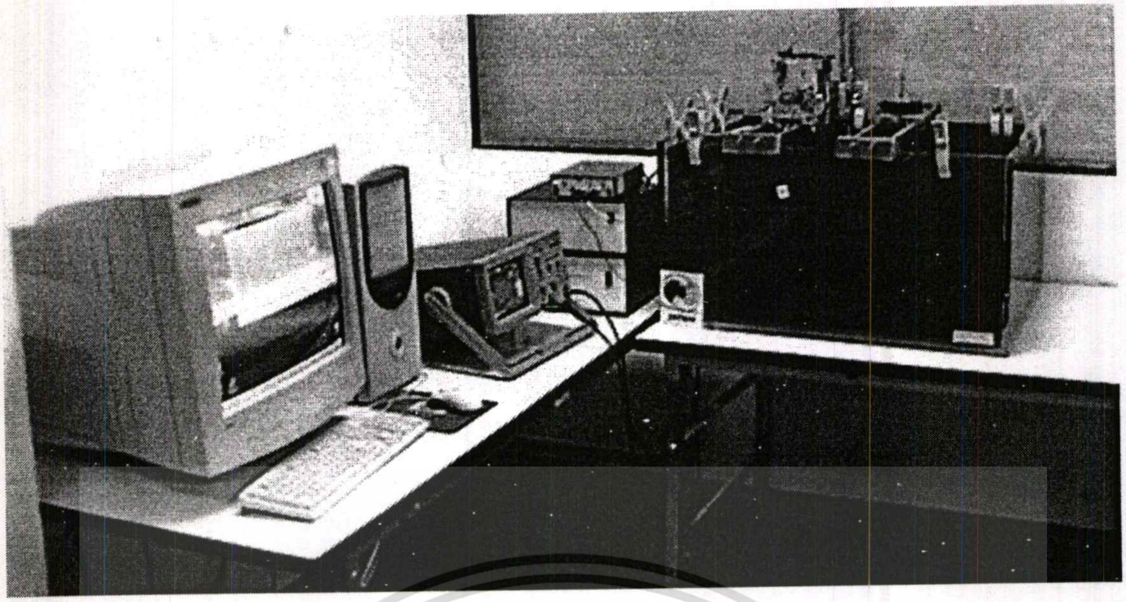

Fig. 4.6 An overview of personal computer is used in our experimental system

4.2 Experimental Estimation of Projections Data from Reflected Data

One main important in this research is the experimental system which concludes the PC used for signals processing including the receiving the signals form oscilloscope. The overview of the experimental system can be show as figure 4.7.

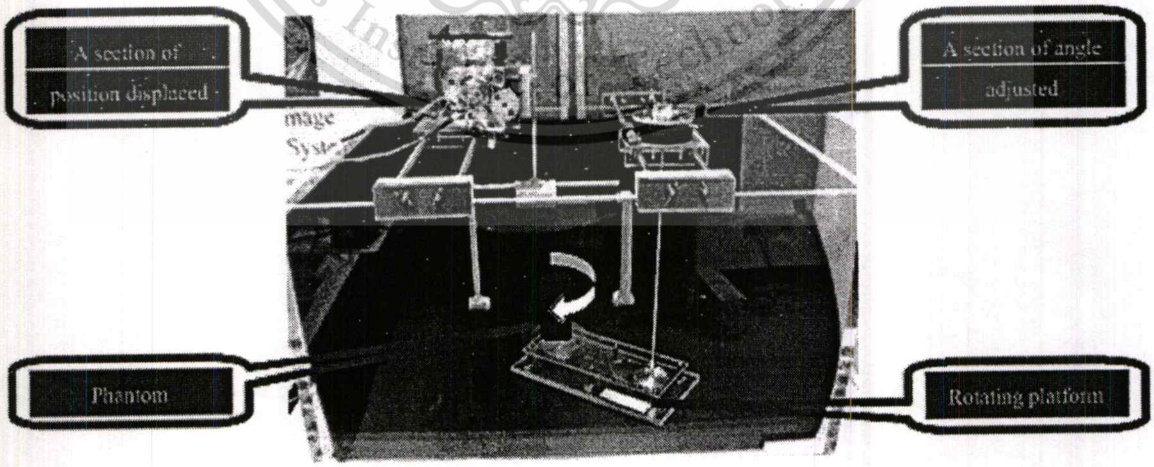

Fig. 4.7 The components in a water tank in our experimental system

This stage consists four main parts:

1. A tested object (phantoms, metals, etc.) is scanned by an ultrasonic transducer mounted on the connecting tools.
2. A section of position displacements (translator stage) works as a holder while a transducer is scanning the tested objects. In addition, a translator shifted 1 mm per every movement of a step motor*.
3. a section of adjusting the angles is used for rotating the object till altogether sufficient angle i.e. 180, 360, or the object characteristic (homogenous or in- homogenous).
4. A section of rotating platform works as a plate for support base of the tested objects. This part is connected to the (3).

4.2.1 Finding the Position of the Ultrasonic Pulse on the Oscilloscope

An estimation of projection data by attenuation measurement can be done by take Fourier transform of the attenuation of the objects which can be obtained from an incident ultrasonic pulse and the latest ultrasonic pulse. Where the incident ultrasonic and the latest ultrasonic pulse can be determined as followed.

The incident ultrasonic pulse can be measured by calculating the distance of ultrasonic pulse from ultrasonic transducer's surface to the first object's layer. The incident ultrasonic pulse can be calculated by referring the sound velocity (appendix A) and the time of ultrasonic pulse from an ultrasonic transducer's surface to the first object's layer. Suppose we know the length from the ultrasonic transducer's surface to the first object's layer 1 cm length, sound velocity of water 15.00 mm/μs. To calculate the position of the wave, we can do as following formula.

Step: $v =$ 1500 mm/μs.

$s =$ 1 cm => 10 mm

$2s = v \times t \Rightarrow t = 2 \times s / v$

2×10 mm / 15.00 mm/μs.

$t = 13.33$ μs. Is the time where the incident pulse.

The reflected ultrasonic pulse can be calculated by referring the sound velocity (from appendix A) and the time of ultrasonic pulse from ultrasonic transducer's surface to the first object's layer plus the sound velocity of ultrasonic passed that metal. For example, $s = v \times t$, then suppose we know the 1cm length from the ultrasonic transducer's surface to the first object's layer, sound velocity of water is 15.00 mm/μs.

4.2.2 Procedure of Projection Estimation from Obtained Data on Simulation

The procedure for estimating the test objects, the incident ultrasonic pulse wave on the simulation can be demonstrated (figure 4.8, figure 4.10). We firstly created the data such as a human's abdomen, an incident ultrasonic pulse wave. After simulating the tested object and the incident ultrasonic pulse wave signal, we then can do a scans. The obtained data can be simulated the results by a purposed method. A frequency-shifted method is applied to the simulated data before applying the purposed method to the experimental data.

A step to the obtained data estimation can be introduced as follow. The simulation of an incident ultrasonic pulse wave and a phantom image as human's abdomen characteristic. The simulated ultrasonic pulse wave is initially synthesized for insonifying the object.

The computer-generated model served as a human's abdomen is shown in figure 4.9, sized 256 by 256 pixels, sampled 1 millimeter per pixel. Each parameters of phantom has the attenuation coefficient of specific value per meter per megahertz $(m.MHz)^{-1}$ respectively.

Table 4.2 Mean Square Error of Reconstruction Images

Center (x, y)	Radius (pixels)	Gray level (0-255)	Alpha
(0,0)	55.95	255	Bone
(0.,-1.27)	53.39	-127	Muscle
(15.29, 0)	14.6	-50	Liver
(-15.29, 0)	19.81	79	Liver
(0., 24.32)	15.95	155	Fat
(0., 6.95)	3.20	124	Spleen
(0., -6.95)	3.20	124	Spleen
(-5.56,-42.05)	3.20	159	Spinal
(0., -42.05)	1.60	159	Spinal
(4.17, -42.05)	2.40	159	Spinal

The table 4.2, data and parameters in table 4.2 are put into C++ programming for creating the phantom model. A procedure of tomographic model designed to simulate the abdomen of the human can be shown as figure 4.8.

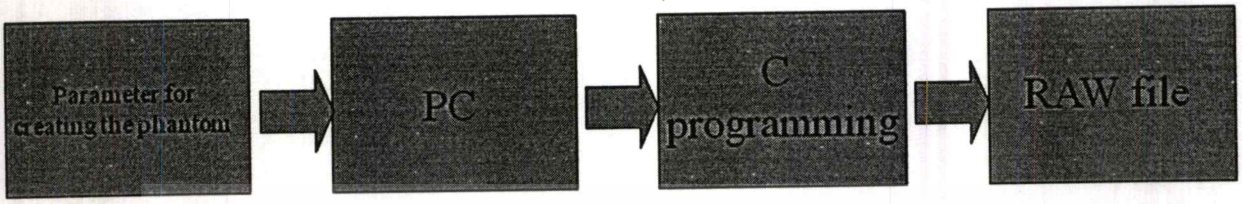

Fig. 4.8 The procedure of tomographic model designed to simulate the abdomen of the human.

After creating the phantom model, the created phantom model is contained as raw data as shown in figure 4.9

Fig. 4.9 The tomographic model designed to simulate the abdomen of the human.

Figure 4.9, the tomographic model created by using the parameters in Table 1, while it is summary of center coordinate of image *(x,y)*, radius in unit *(mm)*, gray level (ρ) is expressed begin from *0* to 1, respectively.

Estimation of incident ultrasonic pulse wave: in the simulation process, the model was issued by the 5 MHz broadband ultrasonic pulse (figure 4.10), sampled at 20 MHz, along the vertical axis. Its latest reflected pulse were then calculated and resolved by the frequency-shifted method to get the value of the integrated attenuation coefficient. We do this repeatedly on the horizontal axis from left to right, we got the array of attenuation coefficients, or called as the projection at the zero angle. Next, the model was rotated by the degrees of two to simulate and obtain the second projection. The process keeps going until we got 90 projections from the half-plane stepping rotation. Subsequently, the model was reconstructed from all of the projections using the simple filtered backprojection algorithm.

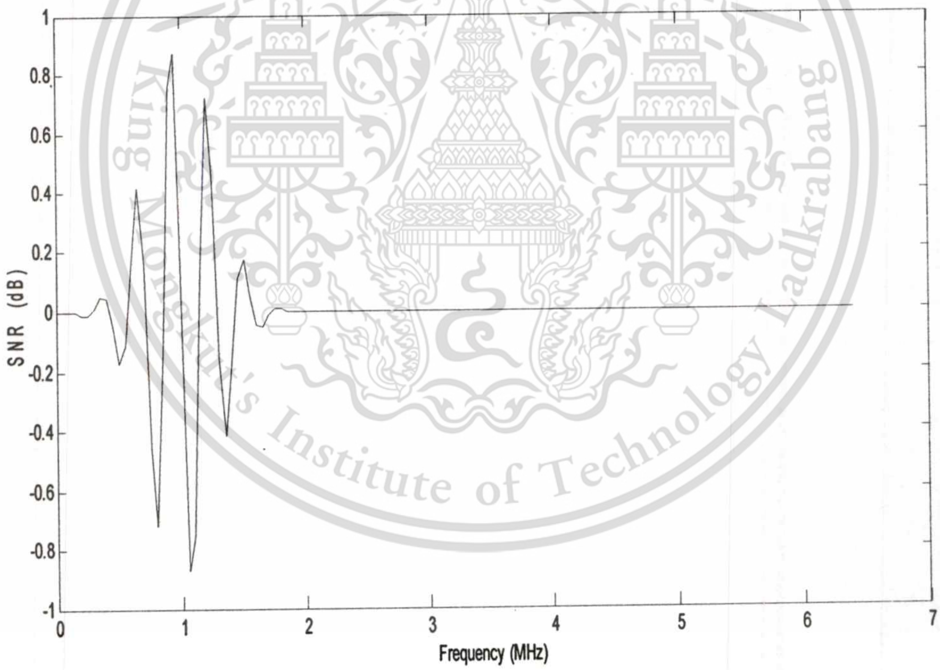

Fig. 4.10 The ultrasonic incident pulse (at 5 MHz frequency)

Figure 4.10 is the incident ultrasonic pulse wave at 5MHz centre frequency, with 20MHz sampling frequency. The X-axis of the figure show frequency in hertz and the Y-axis is the signal to noise ratio in decibel unit.

The Reconstructed Results of a Human's Abdomen

From the results of tested phantom (with signal-to-noise ratio and with noise free) reconstruction, the intersection profiles seems useless because of the absence of details inside the images which are totally blurred from every viewpoint. (see figure. 4.11 (a), (c) for the original images and see figure. 4.11 (b), (d) for the reconstructed images).

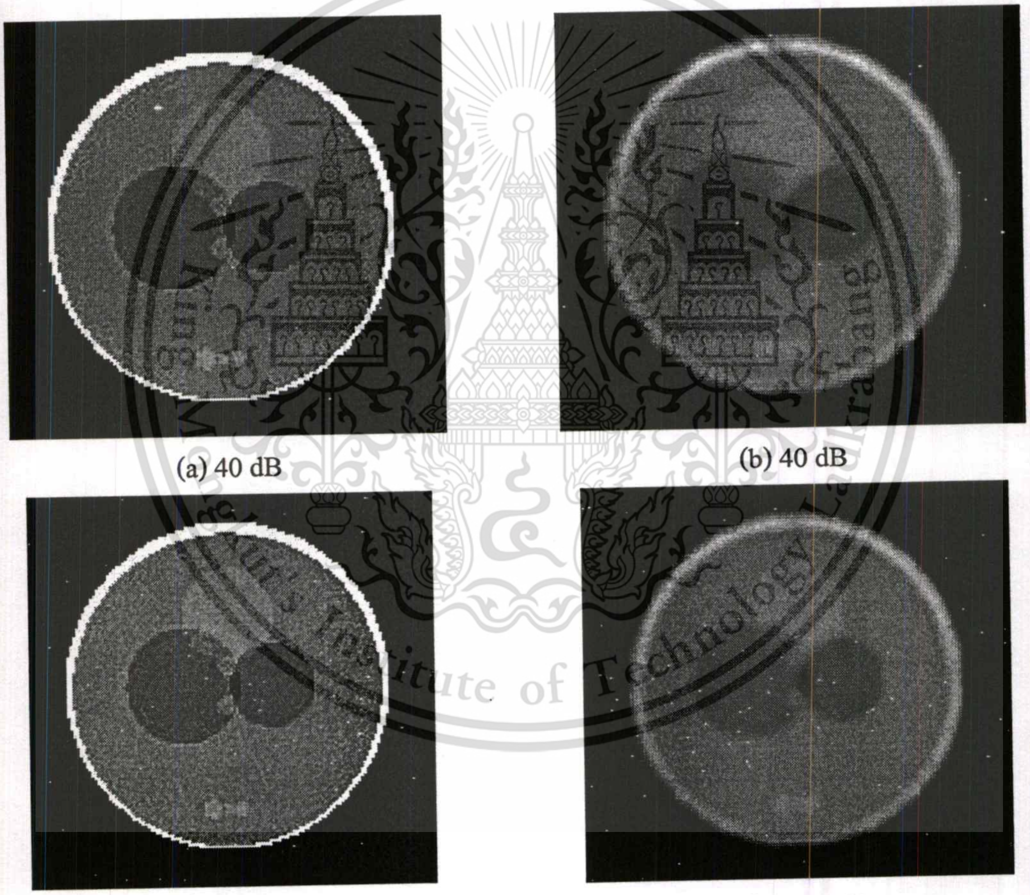

(a) 40 dB (b) 40 dB

(c) 30.45 dB (d) 30.45 dB

Fig. 4.11 Reconstructed image models; (b), (d) are denoted as the reconstructed models; (a), (c) are denoted as the objects with noise models

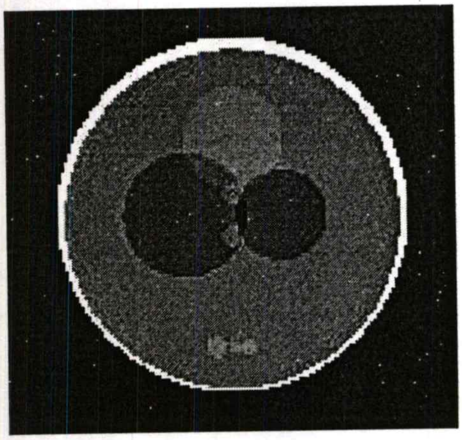

(e) 33.97 dB

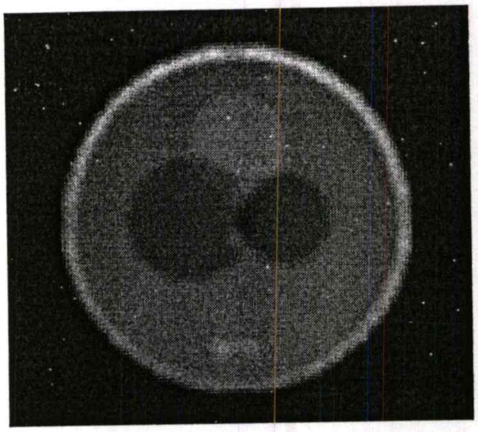

(f) 33.97 dB

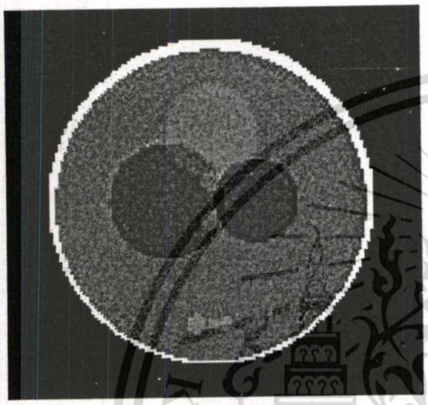

(g) 27.95 dB

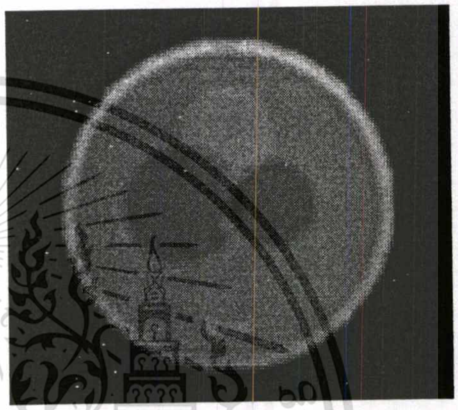

(h) 27.95 dB

Fig. 4.12 Reconstructed image models; (f), (hg) are denoted as the reconstructed models; (e), (g) are denoted as the objects with noise models

To proof whether hat our reconstruction results are accuracy or not, the mean square error formula can help us to provide quantitative of the reconstructed results as shown in figure 4.10 and figure 4.11. The formula can be shown as equation 4.1.

$$MSE = \frac{\sum_{y=0}^{j}\sum_{x=0}^{i}[o(x,y) - o'(x,y)]^2}{\sum_{y=0}^{j}\sum_{x=0}^{i}[o(x,y)]^2} \times 100 \qquad (4.1)$$

In additionally, the MSE values that is used to find the quality and the error of the cross-sectional reconstructed image is shown in Table 4.1

Table 4.1 Mean Square Error of Reconstruction Images

SNR object (dB)	MSE (%)	SNR signal (dB)	MSE (%)
46.0206	17.9672	86.0206	15.9672
40	18.2638	80	16.2638
33.9794	19.2539	73.9794	17.2539
30.4576	20.9578	70.4576	18.9578
27.9588	22.9211	67.9588	19.9211

4.2.3 Procedure of Projection Estimation from Obtained Data on Experiments

UCT using integrated linear slope and the frequency-shifted method initially collect the projections data from sufficient views of the object. The obtained projections data will be calculated by assuming them as linear data.

A Procedure of Projection Estimation from Obtained Data on Experiments: To estimate the projections data from an experimental system, we firstly find the ultrasonic position (an incident ultrasonic pulse wave and the latest reflected ultrasonic pulse wave from the reflected signals from the test object on the oscilloscope). A method is applied to estimate the projection is a frequency-shifted method. An algorithm for finding the specific projections will be purposed as following.

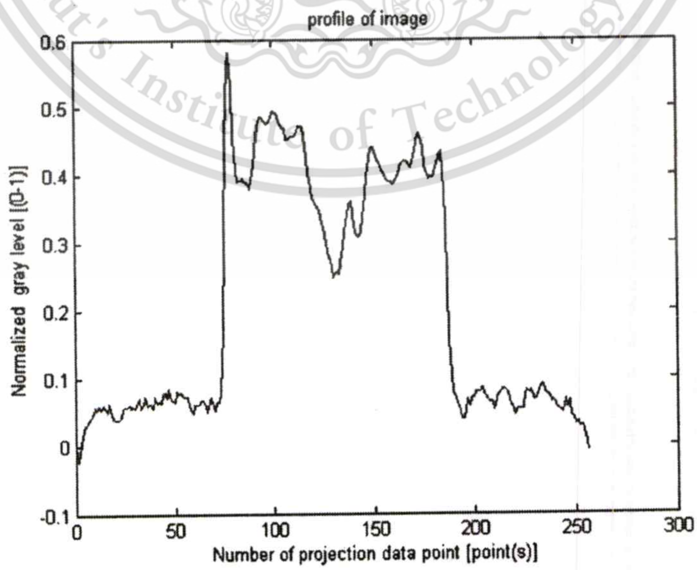

Fig. 4.13 A profile of aluminum data is measured from a aluminum reconstructed result

Figure 4.13 express the aluminum reconstructed detail by showing the profile of reconstructed results. On the left of profile, the amplitude is nearly smoothed because a transmitted signal did not see any object so the gray scale of image assumed as zero while the amplitude of profile is slowly increased when the transmitted signal see the first object interface.

The various data from oscilloscope were transmitted to the PC by using GPIB card interface. Which obtained can be shown as figure 4.13.

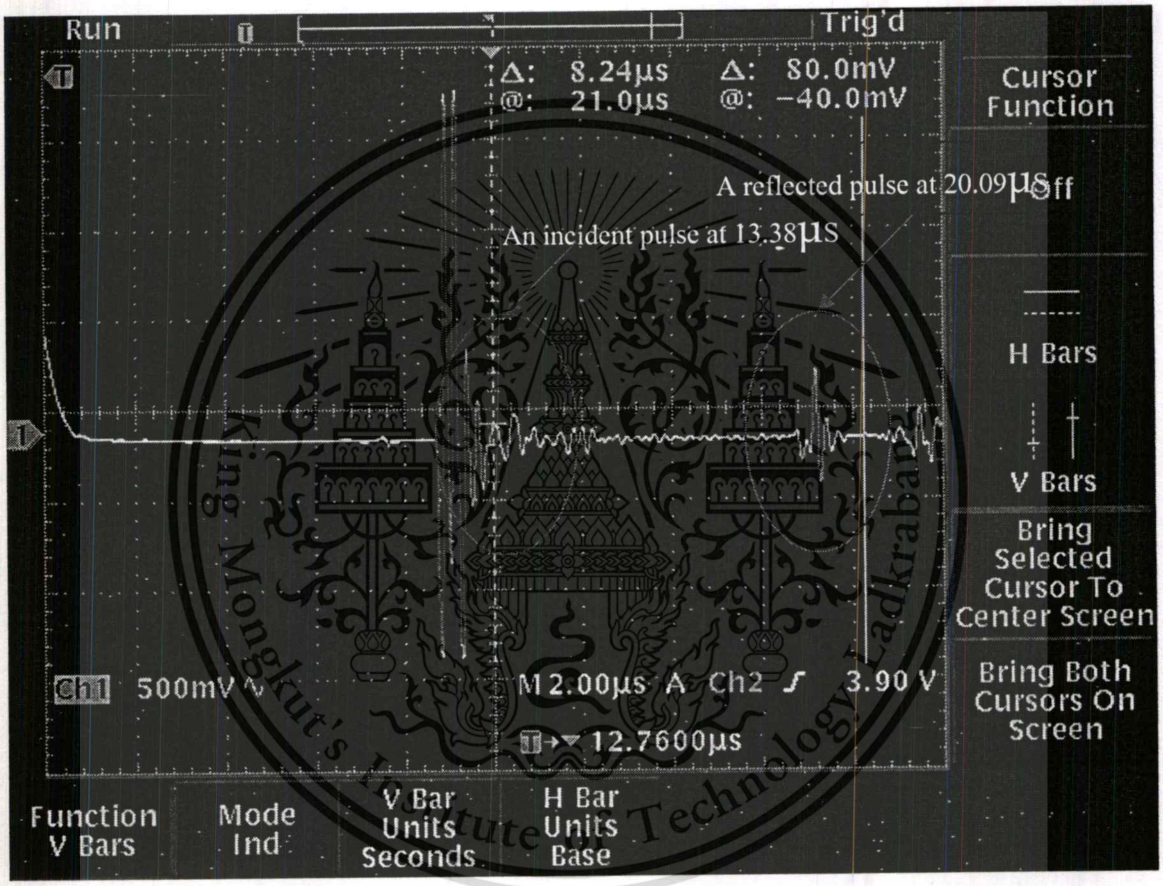

Fig. 4.14 an example of reflected signal of aluminum measured from oscilloscope

Figure 4.14 shows an example of reflected ultrasonic signal from canning the aluminum submerged in water. On a reflected ultrasonic signal, firstly, we take Fourier transform of an incident ultrasonic pulse, a reflected ultrasonic pulse to convert them into frequency domain. Next we take Logarithm both of them. Finally, we can find the attenuation coefficient of the ultrasonic pulse from the object to find the projection data.

4.3.1 The Reconstructed Results of Various Metals

In the reconstructed results of various metals, we see that the reconstructed image details which are not totally blurred from every viewpoint (figure 416, figure 4.17, figure 4.18). This is exactly right since the outer and inner pixels of the reconstructed models are still improved.

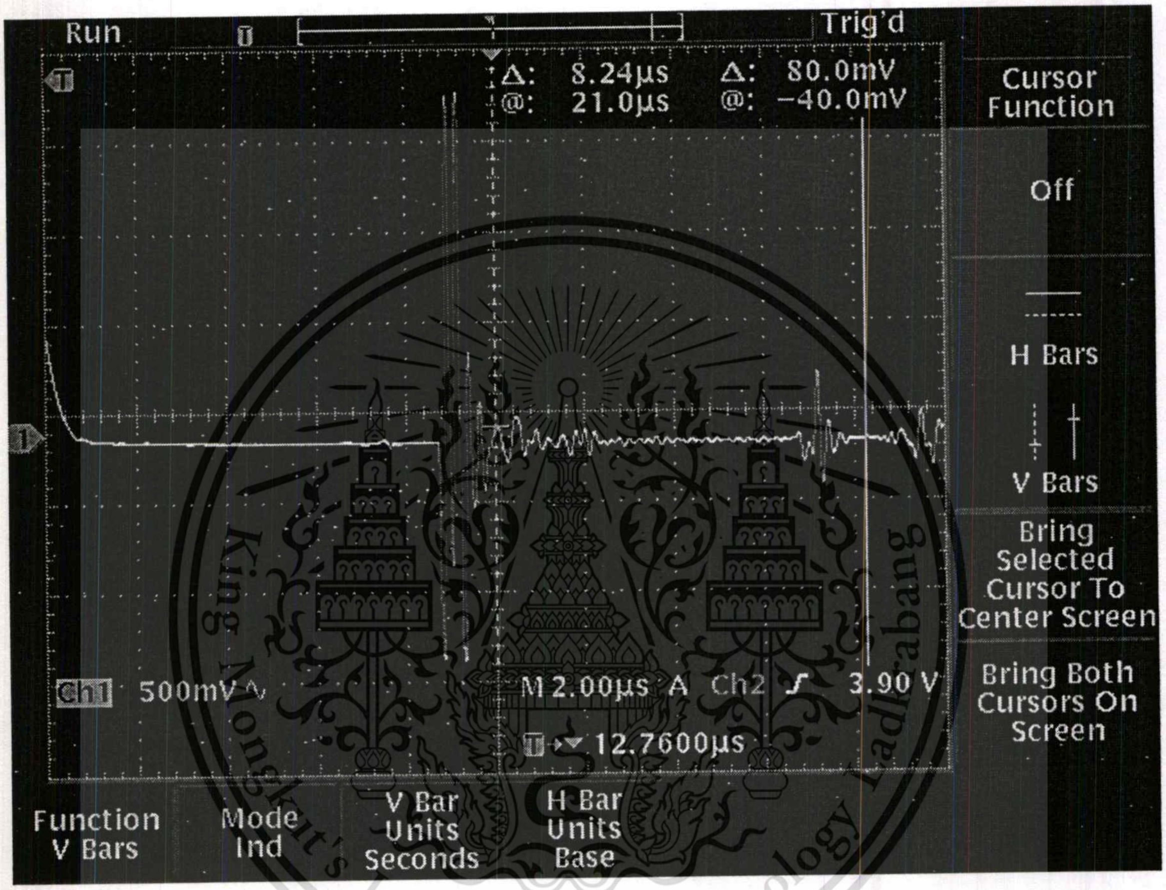

Fig. 4.15 an example of reflected signal of aluminum measured from oscilloscope

There are reconstructed results of various objects such as a rolled steel (with hole), a rolled steel (with non-hole), rolled aluminum (multilayer, with hole) in figure 4.18, figure 4.19, figure 4.20.

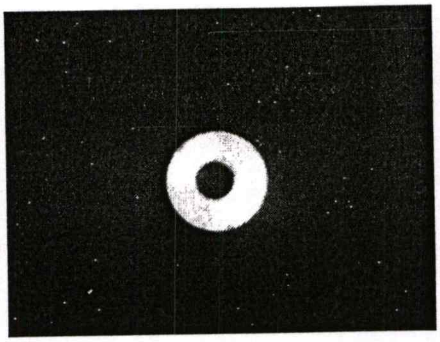

Fig. 4.16 Original rolled steel (with hole)

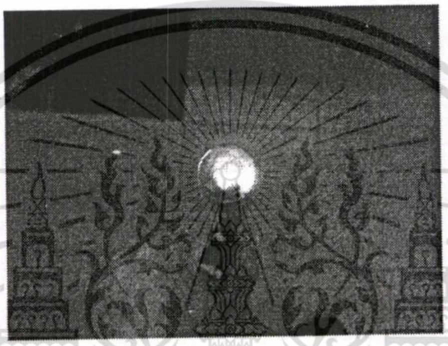

Fig. 4.17 Original rolled steel (with non-hole)

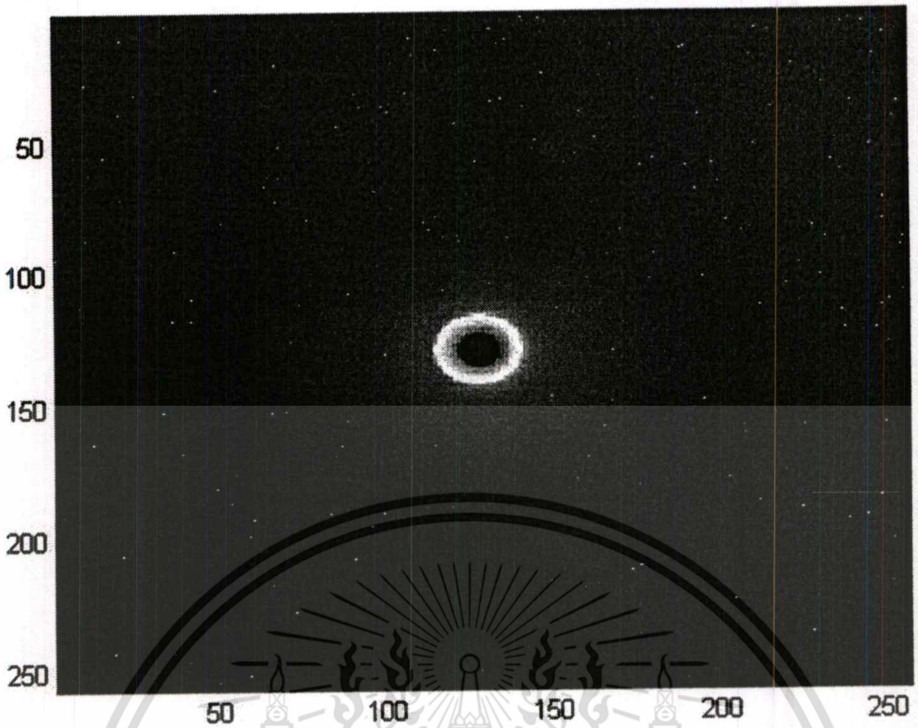

Fig. 4.18 Reconstructed result of rolled steel: steel (with hole)

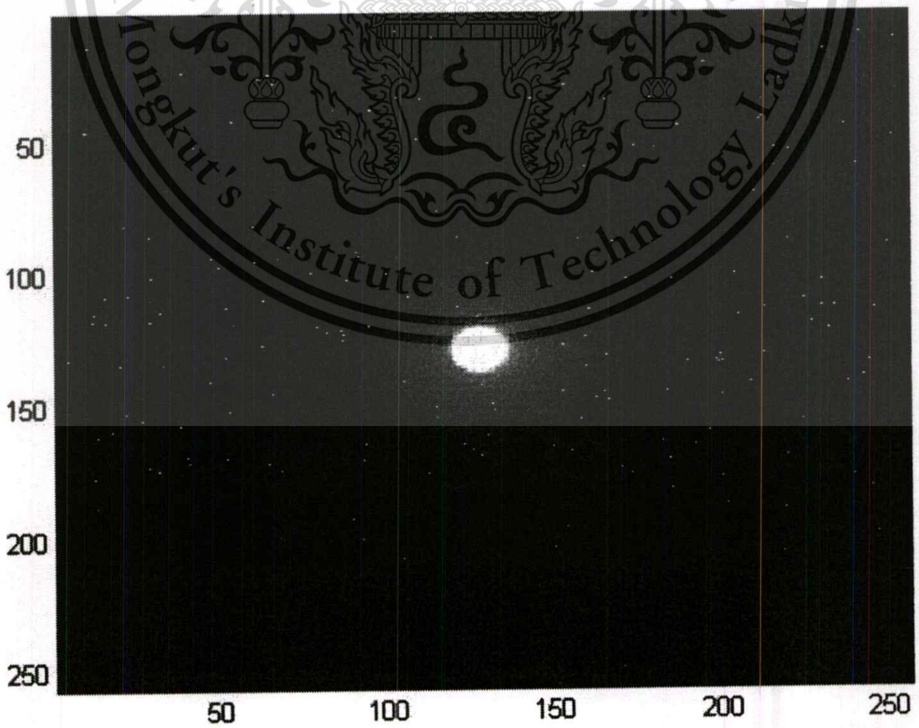

Fig. 4.19 Reconstructed result of rolled steel: steel (with non-hole)

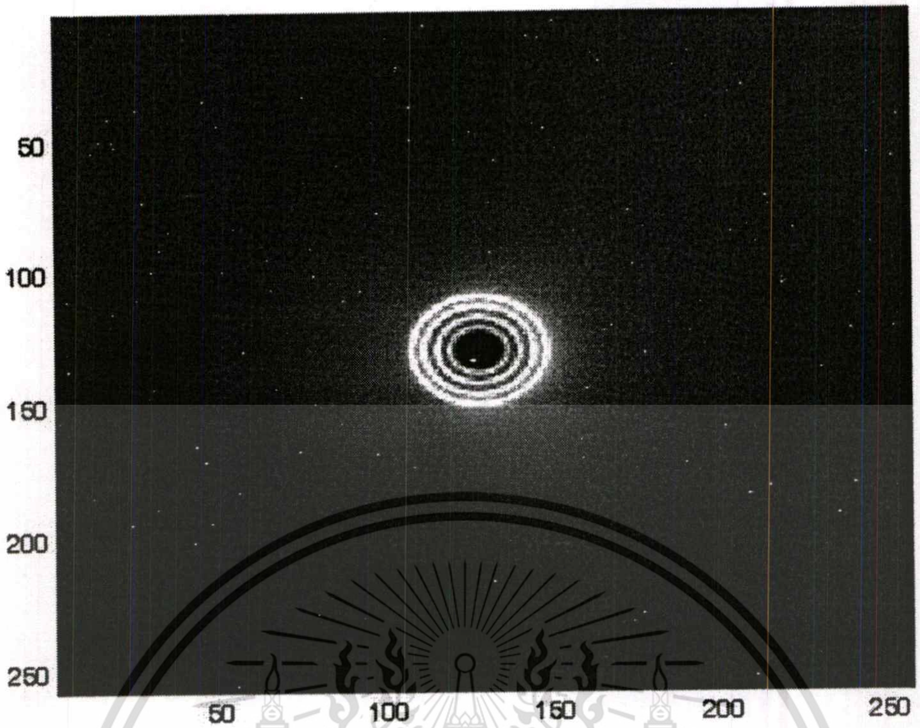

Fig. 4.20 Reconstructed result of rolled aluminum (multilayer, with hole)

In additionally, the MSE values that is used to find the quality and the error of the cross-sectional reconstructed results is shown in Table 4.2

Table 4.2 Mean Square Error of Reconstruction Images

Objects (metals)	Mean square error (MSE) (%)
Rolled steel (with hole)	17.8105
Rolled steel (with non-hole)	18.0972
Rolled aluminum (multilayer, with hole)	19.2902

Chapter 5

Conclusion and Discussion

This thesis, we provide various insights into the knowledge gaps identified in Chapter 1. We focus specifically on how an ultrasonic computed tomography works, especially the ultrasonic reflection-mode tomography using frequency-shifted method. Chapter 2 deals with introducing the ultrasonic general information. Chapter 3 explains about tomographic processes and reconstruction algorithms, starts with the cross-sectional image meaning, parallel beam tomography with parallel beam projection data, filtered backprojection data; ultrasonic computed tomography on two modes concluding transmission-mode and reflection-mode. Chapter 4 shows how a simulation is created and resulted; how to implement with an experimental system.

From the present knowledge it seems, that ultrasound computerized tomography is not useful for imaging of the whole body, but it is suitable for imaging small organs such as mamma infant.

We provide various insights of the related method into the research to achieve the ultrasonic reflection-mode computed tomography using frequency-shifted method. In this attention, the used method was adapted to various types of objects. showing the satisfactory results. In the other hand, we also can assume a linear line scanning as a directed ray and call as the non-diffraction source. Because we assume a ray as a linear scanning line so the scanning line works an x-ray.

Moreover, the system has to be capable of producing images with high resolution and of performing the attenuation measurements. Some clinical measurements will be planed with the combined UTCT/pulse echo scanner that after improvement might find wide clinical utility with mamma and infant imaging in the near future.

In reflection-mode a conventional real-time B-scanner yields B-images with only one linear array. Using ultrasound transmission computed tomography (UTCT) quantitative images of acoustic attention, attenuation slope and acoustic velocity can be obtained by means of two linear arrays in opposition, that are rotated in a plan of the organ. In transmission-mode the transmitted pulses are acquired via a synchronizing and control unit developed by us. The measured projections data are then fed into a personal computer, which calculates the appropriate images.

References

[1] Jofre, L., Hasley, M. S., Broquetas, A., Reyes, E., Ferrando, M. and Elias-fuste, "Medical Imaging with Microwave tomographic Scanner," *IEEE. Trans. Biomed. Eng.*, vol.37. no. 3, pp. 303-312, 1990.

[2] Bolomey, J., -C., "Recent Eurepean Developments in Active Microwave Imaging for Industrial, Scientific, and Medical Application," *IEEE. Trans. Microwave Theory Tech.*. vol. 37., no. 12, pp. 2109-2117, 1989.

[3] Molyneux, J. E. and Witten, A, "Diffraction Tomographic Imaging in a Monostatic Measurement Environment," *IEEE. Trans. Geosci. Remote Sensing*, vol. 31. no. 2, pp. 507-511, 1993.

[4] Faux, S. W., Pele, N. J., Glover, G. H., Gutmann, F. D., and Mclachlan, M., "Spectral Characteristics and Attenuation Measurements in Ultrasound," *Ultrason. Imaging*, vol. 5, pp. 95-116, 1983.

[5] Kuc, R., "Estimating Acoustic Attenuation from Reflected Ultrasound Signals: Comparison of Spectral- Shift and Spectral-Difference Approaches," *IEEE Trans. Acoust. Speech Signal Processing*, vol. ASSP-32, pp. 1-7, 1994.

[6] Nielsen, S.A. and Andersen, S.I.: *18th Riso Intern. Symp. on Materials Science*, 1997,1:455-464.

[7] G. Tangtisanon and K.Jaruwongrunsee, "Ultrasonic Diffraction Tomography by Pulse-Plane Wave: Experimental Result by Frequency Synthesis Method," Proceedings of the 2005 IEEĖ, Engineering in Medicine and Biology 27th Annual Conference. Shanghai, China, September 1-4, 2005, pp 1822-1825.

[8] K. Jaruwongrungsee, "Transmission Mode Ultrasonic Tomography using Generalized Fourier Transform," Master Thesis, KMITL, Thailand.

[9] http://www.cs.sunysb.edu/~mueller/teaching/cse377/ultrasound.pdf

[10] http://www.lsp.open.ac.uk/teachcupbrd/physics4/ultrasound.ppt.

[11] PANAMETRICS, INC. Phone (781) 899-2719 • Fax (781) 899-1552 • Website: www.panametrics.com • E-mail: ndt@panametrics.com

[12] Medical Imaging Physics, Fourth Edition, by William R. Hendee and E. Russell Ritenour ISBN: 0-471-38226-4 Copyright C_ 2002 Wiley-Liss, Inc.

[13] K. Hamamoto, B. Andreas, T. Shiina, and M. Ito, "Basic Investigation on Reflection Mode Ultrasonic Attenuation Tomography", Jpn. J. Appl. Phys., Japan, vol. 34 (May 1995), pp. 2812-2816.

[14] http://cat.inist.fr/?aModele=afficheN&cpsidt=3601540

[15] B. J. Oosterveld, J. M. Thijssen, P. C. Hartman, R. L. Romijn, and G. J. E. Rosenbusch. \Ultrasound attenuation and texture analysis of di_use liver disease: Methods and preliminary results," Phys. Med. Biol. 36, pp. 1039{1064. aug 1991.

[16] J. M. Girault. F. Ossant, A. Ouahabi, C. Guittet, D. Kouam_e, and F. Patat, \Non-stationary parametric spectral estimation for ultrasound attenuation," Acoustical Imaging 23, pp. 53{59, 1997.

[17] M. Fink, F. Hottier, and J. F. Cardoso, \Ultrasonic signal processing for in vivo attenuation measurement: Short time Fourier analysis," Ultrasonic Imaging 5(2), pp. 117{135, 1983.

[18] K. A. Dines, and A. C. Kak, "Ultrasonic Attemuation Tomography of Soft Biological Tissues", Ultrason. Imaging, vol. 1, 1979, pp. 16-33.

[19] eBook, B.G. Batchelor and P.F. Whelan, "Intelligent Vision Systems for Industry" © Bruce G. Batchelor, Paul F. Whelan 2002, Previously published in hardback by Springer-Verlag (ISBN 3-540-19969-1) in 1997.

[20] [20a] S. J. Norton and M. Linzer, "Ultrasonic reflectivity tomography: Reconstruction with circular transducer arrays," Ultrason. Imaging, vol. 1, no. 2, pp. 154-184, Apr. 1979.

[20b]-, "Ultrasonic reflectivity tomography in three dimensions: Reconstruction with spherical transducer arrays," Ultrason. Imaging, vol. 1, no. 2, pp. 210-231, 1979.

[21] "What is HPIB · GPIB · IEEE 488 · IEC 60625 ?", http://www.ines.de/gpib-info.html

[22] K. Hamamoto, " Basic Investigation on Reflection Mode Ultrasonic Attenuation Tomography, " Jpn. J. Appl. Phys. Vol 34 (1995) pp. 2812-2816, Part 1, No. 5B, May 1995.

[23] T. Onemanisone, C. Pintavirooj, K. Wong-ek, S. Sangworasilp, "Ultrasonic Reflection Tomography using Frequency Centroid-Shift Method," the 2007 ECTI International Conference (ECTI2007), Chiang Rai, Thailand, pp 1073-1076, 9-12, May 2007.

Appendix A

Some Properties of the Objects

In consideration of ultrasonic attenuation α_0 in the water we can see that, the ultrasonic attenuation is very low when we compare the ultrasonic attenuation in water to ultrasonic attenuation in other medium.

To show some of ultrasonic attenuation in some specific objects in a table A.1 [3] as below; the attenuated ultrasound of water can be ignored.

Table A.1 Sound velocity and objects attenuation coefficients

Medium	Velocity (m/sec)	Attenuation coefficient
Air	343	1.38
Water	1484	0.00025
Blood*	1550	0.02
Myocardium*	1550	0.35
Fat*	1450	0.06
Liver*	1570	0.11
Kidney*	1560	0.09
Bone	3360	1.3

Note: * = soft tissue

Table A.2 the tissue characteristic impedance and attenuation at 1 MHz

Tissue	Characteristic Impedance $\rho_0 c \left(10^6 Ns/m^3\right)$	Attenuation at 1 MHz (dB/cm)
Blood*	1-62	0.2
Spleen	1-6	0.4
Liver*	1.65	0.7
Fat*	1-38	0.8
Brain*	1-60	0.8
Muscle*	1.65-1.74	1.5-2.5
Bone	3.2-7.4	11
Lung*	0.26-0.46	40
Water	1.49	0.0025

Note: * = soft tissue

Table A.2 introduces the characteristic impedance and attenuation of the tissues for the specific frequency at 1 MHz.

Note that, in calculating the characteristic impedance and the ultrasonic attenuation, the useful units are introduced. The units for the characteristic impedance and the ultrasonic attenuation are $\rho_0 c\left(10^6\ Ns/m^3\right)$ and dB/cm), respectively.

In addition, when an ultrasonic wave travels through the specific object then results a longitudinal velocity. That is a longitudinal velocity of ultrasound which used to find the time of ultrasonic pulse wave position. One important component in finding the position of the ultrasonic pulse on the oscilloscope is longitudinal velocity.

Table A.3 Sound velocity in materials

Material	Longitudinal Velocity (mm/μs)	Longitudinal Velocity (m/s)
Aluminum	6.350	6350
Brass	4.430	4430
Copper	4.700	4700
Plexiglas	2.680	2680
Stainless	5.610	5610
Steel	5.940	5940
Water	1.494	1494

In object thickness measurement can be done by the sound velocities and sound distances passed through the objects shown as below equation 4.8

$$S = v \times t$$

Where

S is the ultrasonic traveling path length (m).

v is the ultrasonic velocity passed through the water (m/s).

t is the ultrasonic periods (s).

Autobiography

Born in Vientiane on October 19, 1983, I received the bachelor's degree of engineering (Electronics) from National University of Laos in 2004. Afterwards, I enrolled in the master course of engineering at King Mongkut's Institute of Technology, Ladkrabang in 2005. with the major in electronics. In addition, I worked as a researcher for the project of *Image Reconstruction from Ultrasonic Wave,* and an instructor for the undergraduates in the electronic laboratory.

The publications I have submitted during the master course are as follows:

[i] C. Pintavirooj C. Pintavirooj*, T. Onemanisone*, K. Jaruwongrungsee*, K. Hamamoto*** and W. Withayachumnankul** , "ULTRASONIC DIFFRACTION TOMOGRAPHY WITH MULTIPLE FREQUENCY SYNTHESIS ," *Proc.* The 12 th International Conference On Biomedical Engineering 7 – 10 December 2005, Suntec Singapore International Convention & Exhibition Centre, SINGAPORE. pp. 377-380.

[ii] P. Tosranont, T. Onemanisone*, P. Greesuradej, C. Pintavirooj, K. Jaruwongrungsee*, " Ultrasonic Reflection Mode Tomography Using Frequency-Shift Method", International Symposium on Communications And Information Technologies 2006 (ISCIT 2006), October 18-20, 2006 Grand Mercure Fortune Hotel, Bangkok, Thailand, pp. 835-838.

[iii] T. Onemanisone 1 , C. Pintavirooj 1 , K. Jaruwongrungsee 1 and Manas Sangworasil 1,2, "Comparison Study of Ultrasonic Diffraction Tomography and Ultrasonic Non-Diffraction Tomography, " *Proc.* World Congress, Soul Korea. pp. 2429-2432

[iv] T. Onemanisone " Ultrasonic Reflection Mode Tomography using Frequeency Centroid Shifted Method," *Proc. ECTI-CON 2007*, 9-12 May 2007, Mea Fah Laung University, Chiangrai, Thailand.

Any comment or query should be sent directly to thongsone82@gmail.co.th